The Influence of Carbon Cycling on Oxygen Depletion in North-Temperate Lakes

Austin Delany[1], Robert Ladwig[1], Cal Buelo[1], Ellen Albright[1], Paul C. Hanson[1]

[1] Center for Limnology, University of Wisconsin-Madison, Madison, WI, USA

Correspondence to: Austin Delany (addelany@wisc.edu)

Abstract. Hypolimnetic oxygen depletion during summer stratification in lakes can lead to hypoxic and anoxic conditions. Hypolimnetic anoxia is a water quality issue with many consequences, including reduced habitat for cold-water fish species, reduced quality of drinking water, and increased nutrient and organic carbon (OC) release from sediments. Both allochthonous and autochthonous OC loads contribute to oxygen depletion by providing substrate for microbial respiration; however, their relative contributions to oxygen depletion across diverse lake systems remains uncertain. Lake characteristics, such as trophic state, hydrology, and morphometry are also influential in carbon cycling processes and may impact oxygen depletion dynamics. To investigate the effects of carbon cycling on hypolimnetic oxygen depletion, we used a two-layer process-based lake model to simulate daily metabolism dynamics for six Wisconsin lakes over twenty years (1995-2014). Physical processes and internal metabolic processes were included in the model and were used to predict dissolved oxygen (DO), particulate OC (POC), and dissolved OC (DOC). In our study of oligotrophic, mesotrophic, and eutrophic lakes, we found autochthony to be far more important than allochthony to hypolimnetic oxygen depletion. Autochthonous POC respiration in the water column contributed the most towards hypolimnetic oxygen depletion in the eutrophic study lakes. POC water column respiration and sediment respiration had similar contributions in the mesotrophic and oligotrophic study lakes. Differences in source

of respiration are discussed with consideration of lake productivity and the processing and fates of organic carbon loads.

1 Introduction

Hypolimnetic oxygen depletion is a persistent and global phenomenon that degrades lake ecosystems services (Nürnberg 1995; Cole & Weihe 2016; Jenny et al. 2016). In lakes where oxygen depletion results in hypoxia and even anoxia, habitat availability for cold-water fish species is eliminated (Magee et al. 2019), quality of drinking water is reduced (Bryant et al. 2011), and nutrient and OC release from lake sediments becomes elevated (Hoffman et al. 2013, McClure et al. 2020). An increase in the prevalence of hypolimnetic anoxia and associated water quality degradation in temperate lakes indicates the need to better understand how lake ecological processes interact with external forcings, such as hydrology and nutrient inputs, to control the development of anoxia (Jenny et al, 2016 a,b).

Allochthonous organic carbon (OC) loading to lakes that explains the prevalence of negative net ecosystem production (i.e., net heterotrophy) provides substrate for hypolimnetic oxygen depletion (Houser et al. 2003). Allochthonous OC sources have also been shown to influence dissolved oxygen (DO) and carbon dynamics in lakes by providing recalcitrant substrate for respiration (Cole et al. 2002; Hanson et al. 2014, Solomon et al. 2015). In lake surveys, dissolved allochthonous OC correlates positively with net heterotrophy ((Jansson et al. 2000), indicating the importance of allochthony to both the carbon balance and dynamics of dissolved gases (Prairie et al. 2002; Hanson et al. 2003). However, the persistent and often stable concentration of allochthonous DOC in the water column of lakes also indicates its recalcitrant nature, raising the question of whether allochthony alone can support high oxygen demand in the sediments and deeper waters of lakes.

The contributions of OC from autochthony to hypolimnetic oxygen depletion may be important as well, despite its low concentrations relative to that of allochthonous OC in many lakes (Cole et al. 2002). Autochthonous OC tends to be highly labile (Amon & Brenner 1996, Thorpe & Delong 2002), and spot samples from lake surveys may not detect autochthonous DOC, reducing its power as a correlate of ecosystem function. Positive correlation between anoxia and lake phosphorus concentrations suggests autochthony may contribute substantially to hypolimnetic oxygen demand (Rhodes et al. 2017; Rippey & McSorley, 2009; Jenny et al. 2016a,b); however, the link between nutrient concentrations, autochthony, and hypolimnetic respiration is rarely quantified. Lakes with high autochthony can still be net heterotrophic (Staehr et al. 2010; Cole et al. 2000), however, it matters where in the lake autochthony is respired. Export of phytoplankton from the epilimnion to the hypolimnion and sediments contributes to deep water oxygen demand (Müller et al. 2012; Rhodes et al. 2017; Beutel 2003), and the magnitude and timing of organic carbon inputs to deeper waters in lakes and the subsequent fate of that carbon deserves further exploration.

Understanding the relative contributions of autochthony and allochthony to hypolimnetic oxygen depletion requires consideration of a number of physical and biological processes controlling oxygen sources and sinks in lakes (Hanson et al. 2015). For dimictic north temperate lakes, the timing and dynamics of seasonal stratification determine the ambient temperature and light conditions for metabolism and the extent to which the hypolimnion is isolated from oxygen-rich surface waters (Snortheim et al. 2017, Ladwig et al. 2021). In many lakes, the hypolimnion is below the euphotic zone, but in very clear lakes, primary production within the hypolimnion may be an oxygen source (Houser et al. 2003). Lake

morphometry influences the spatial extents of stratified layers, which determines the ratio of hypolimnetic volume to sediment surface area and the magnitude the sediment oxygen sink for the hypolimnetic oxygen budget (Livingstone & Imboden 1996). Thus, the sources and labilities of OC, lake morphometry, and lake hydrodynamics all contribute to hypolimnetic oxygen budgets, making it an emergent ecosystem property with a plethora of causal relationships to other ecologically important variables.

The availability of long-term observational data combined with process-based models provides an opportunity to investigate OC sources and their control over the dynamics of lake DO across multiple time scales. Long-term studies of lakes on regional and global scales highlight how environmental trends can influence metabolic processes in lakes, and how lakes can broaden our understanding of large-scale ecosystem processes (Richardson et al. 2017, Kraemer et al. 2017, Williamson et al. 2008). For example, long-term studies allow us to investigate the impact that current and legacy conditions have on lake ecosystem function in a given year (Carpenter et al. 2007). Process-based modeling has been used to investigate metabolism dynamics and understand both lake carbon cycling (Hanson et al. 2004, Cardille et al. 2007) and formation of anoxia (Ladwig et al. 2021); however, explicitly tying lake carbon cycling and metabolism dynamics with long-term hypolimnetic DO depletion across a variety of lakes remains largely unexplored. The combination of process-based modeling with available long-term observational data, including exogenous driving data representative of climate variability, can be especially powerful for recreating representations of long-term lake metabolism dynamics (Staehr et al. 2010, Cardille et al. 2007).

In this study, our goal is to investigate OC source contributions to lake carbon cycling and hypolimnetic oxygen depletion. The importance of excess primary production to anoxia has been established (Nürnberg et al. 1995, Müller et al. 2012). We build upon this research by quantifying the timing and magnitude of OC contributions to hypolimnetic anoxia. We are particularly interested in the relative loads of autochthonous and allochthonous OC to lakes and how they contribute to hypolimnetic DO depletion across seasonal to decadal scales. We use a process-based lake metabolism model, combined with daily external driving data and long-term limnological data, to study six lakes within the North Temperate Lakes Long-Term Ecological Research network (NTL LTER) over a twenty-year period (1995-2014). We address the following questions: (1) What are the dominant sources of organic carbon that contribute to hypolimnetic oxygen depletion, and how do their contributions differ across a group of diverse lakes over two decades? (2) How does lake trophic state influence the processing and fates of organic carbon loads in ways that affect hypolimnetic dissolved oxygen?

2 Methods

2.1 Study Site

This study includes six Wisconsin lakes from the NTL-LTER program (Magnuson et al. 2006). Trout Lake (TR), Big Muskellunge Lake (BM), Sparkling Lake (SP), and Allequash Lake (AL) are in the Northern Highlands Lake District of Wisconsin and have been regularly sampled since 1981 (Magnuson et al. 2006). Lake Mendota (ME) and Lake Monona (MO) are in southern Wisconsin and have been regularly sampled by the NTL-LTER since 1995

(NTL-LTER, Magnuson et al. 2006). The NTL-LTER provides a detailed description of each lake (Magnuson et al. 2006). The six lakes span gradients in size, morphometry, landscape setting, and hydrology, which creates diverse carbon cycling characteristics and processes across these systems. TR and AL are drainage lakes with high allochthonous carbon inputs from surface water, while BM and SP are groundwater seepage systems with allochthony dominated by aerial OC inputs from the surrounding landscape (Hanson et al. 2014). All four northern lakes (TR, AL, BM, SP) are surrounded by a forested landscape. ME and MO are both eutrophic drainage lakes surrounded by an urban and agricultural landscape. Although the full range of DOC concentrations for lakes in northern Wisconsin varies from about 2 to >30 mg L^{-1} (Hanson et al. 2007), DOC concentrations among our study lakes covered a relatively narrow range typical of non-dystrophic lakes in Wisconsin (Hanson et al. 2007) and are near the global averages previously estimated, i.e., 3.88 mg/L (Toming et al. 2020) and 5.71 mg/L (Sobek et al. 2007), respectively. Morphometry, hydrology, and other information can be found in Table 1.

Table 1. Physical and biogeochemical characteristics of the study lakes. The table includes lake area (Area), maximum depth (Zmax), hydrologic residence time (RT), mean annual temperature (Temp), mean annual surface total phosphorus concentration (Mean TP), and mean annual surface DOC (Mean DOC).

Lake	Area (ha)	Zmax (m)	RT [3,4] (years)	Temp [2] (°C)	Mean TP [1] (µgL)	Mean DOC [1] (mgL)
Allequash Lake (AL)	168.4	8	0.73	10.5	14	3.9
Big Muskellunge (BM)	396.3	21.3	5.1	10.5	7	3.8
Sparkling Lake (SP)	64	20	8.88	10.6	5	3.12
Trout Lake (TR)	1607.9	35.7	5.28	9.8	5	2.8
Mendota (ME)	3961	25.3	4.3	12.5	50	5.6
Monona (MO)	1324	22.5	0.7	13.8	47	5.8

1 - Magnuson et al. (2020, 2006)
2 - Magnuson et al. (2022)
3 - Hunt et al. (2013)
4 - Webster et al. (1996)

2.2 Driving Data and Limnological Data

Most driving data for the model is provided by the "Process-based predictions of water temperature in the Midwest US" USGS data product (Read et al. 2021). This includes lake characteristic information such as lake area and hypsometry, daily modeled temperature

profiles, ice flags, meteorology data, and solar radiation for the six study lakes. Derived hydrology data is used in calculating daily OC loading and outflow for the study lakes. Hydrology for the northern lakes is taken from Hunt & Walker (2017), which was estimated using a surface and groundwater hydrodynamic model. Hydrology for ME is taken from Hanson et al. (2020), which used the Penn State Integrated Hydrologic Model (Qu & Duffy 2007). We assume for ME and MO that evaporation from the lake surface is approximately equal to precipitation on the lake surface and that groundwater inputs and outputs to the lake are a small part of the hydrologic budgets (Lathrop & Carpenter 2014). Therefore, ME outflow is assumed to be equal to ME inflow. ME is the predominant hydrologic source for MO (Lathrop & Carpenter 2014), thus, MO inflow is assumed to be equal to ME outflow, and MO outflow is assumed to be equal to MO inflow. We found that the derived discharge data for ME, TR, AL, and SP was approximately 20-50% higher than previously reported values (Hunt et al. 2013, Webster et al. 1996), depending on the lake, while hydrology in BM was approximately 25% too low (Hunt et al. 2013). To accommodate this issue, we adjusted total annual hydrological inputs to match published water residence times for each lake (Table 1), while retaining temporal hydrological patterns. NTL-LTER observational data are interpolated to estimate daily nutrient concentration values, which are used in calculating daily primary production in the model (Magnuson et al. 2020).

The NTL-LTER observational data used to calibrate and validate the model for the six lakes include DO, DOC, and Secchi depth (Magnuson et al. 2020, Magnuson et al. 2022). Saturation values for DO and gas exchange velocity used in calculating atmospheric

exchange for DO are calculated using the "o2.at.sat.base" and using the Cole and Caraco gas exchange method from the "K600.2.KGAS.base" function within the USGS "LakeMetabolizer" package in R (Winslow et al. 2016).

2.3 The Model

The goal of our model is to use important physical and metabolic processes involved in the lake ecosystem carbon cycle to best predict DO, DOC, and POC, while keeping the model design simple in comparison with more comprehensive water quality models (e.g., Hipsey et al. 2022). We ran our model with a daily time step over a twenty-year period (1995-2014) for each lake and included seasonal physical dynamics, such as lake mixing, stratification, and ice cover from Read et al. 2021. Throughout each year, the model tracks state variables and fluxes in the lake for each day (Fig. 1). These state variables include DO and the labile and recalcitrant components of particulate organic carbon (POC) and dissolved organic carbon (DOC). Initial conditions for each state variable are based on literature values or lake observational data (SI Table 5). The model is initialized on January 1st of the first year, so we set the initial labile POC mass to zero under the assumption that the concentration is low in the middle of winter. The initial DO value is set to the saturation value based on the conditions of the initial model run day and is calculated using the LakeMetabolizer R package (Winslow et al. 2016). During stratified periods, the state variables and fluxes for the epilimnion and hypolimnion are tracked independently. Atmosphere, sediments, and hydrologic inputs and outputs are boundary conditions.

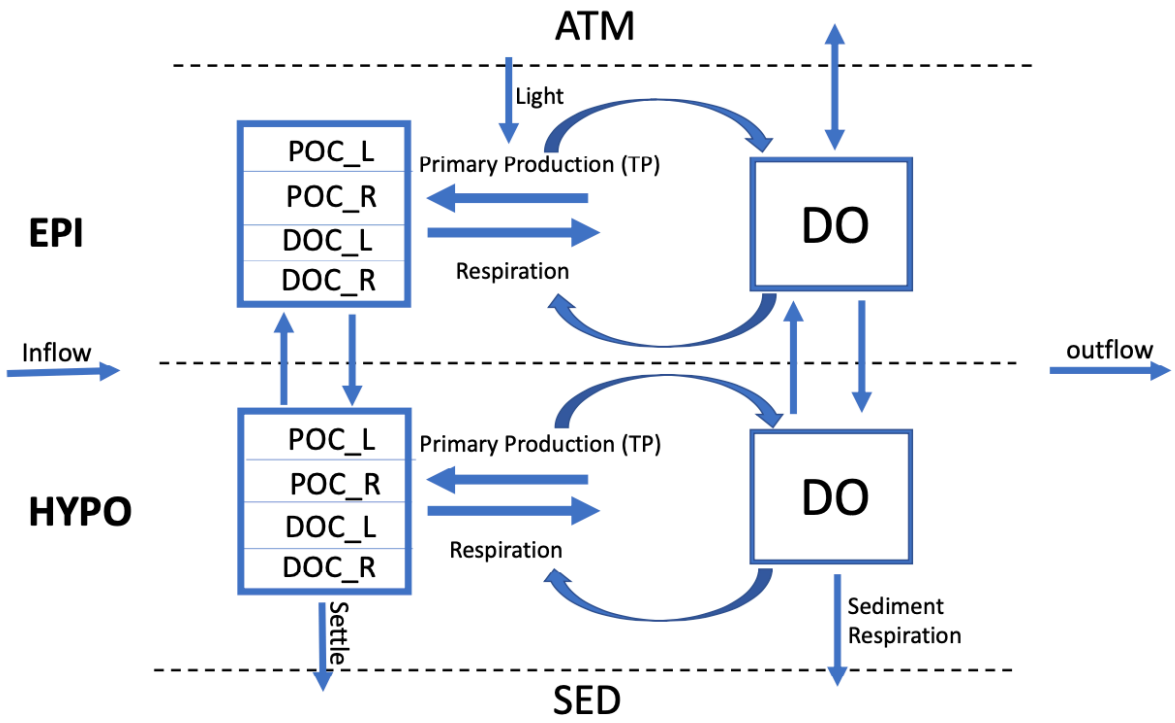

Figure 1. Conceptual lake model showing state variables (boxes) and fluxes (arrows). The model has two thermal layers under stratified conditions, as shown here, and tracks state variables separately for each layer. The sediment (SED), atmosphere (ATM), inflow and outflow are system boundaries. The state variables included are DO (dissolved oxygen), DOC_L (labile dissolved organic carbon), DOC_R (recalcitrant dissolved organic carbon), POC_L (labile particulate organic carbon), and POC_R (recalcitrant particulate organic carbon). Observed total phosphorus (TP) is used as a driving variable for primary production in the model.

The model is built specifically for this analysis; however, many of the assumptions around the model complexity and mathematical formulations are borrowed from literature cited (Ladwig et al. 2021, Hipsey et al. 2022, Hanson et al. 2014, McCullough et al. 2018). We chose to develop our own process-based model for water quality rather than use an existing model, such as GLM-AED2 (Hipsey et al. 2022; note that AED2 is the water quality component of the coupled hydrodynamic-water quality model) or Simstrat (Goudsmit et al. 2002), so that we could simulate and measure the specific metabolism fluxes related to our study questions. We used a pre-existing dataset (Read et al. 2021) that provided GLM

263 modeled daily water temperature profiles for our study lakes, however our study did not use
264 any established water quality models to calculate the relative OC or DO pools.
265
266 **2.3.1 Stratification Dynamics**
267 Lake physical dynamics are taken from the output of a previous hydrodynamic modeling
268 study on these same lakes over a similar time period (Read et al. 2021), which used the
269 General Lake Model (Hipsey et al. 2019). Before running the metabolism model, a
270 thermocline depth for each time step is estimated using derived temperature profiles for each
271 lake (Read et al. 2021) by determining the center of buoyancy depth (Read et al. 2011). After
272 calculating the thermocline depth, the volumes and average temperatures for each layer, and
273 the specific area at thermocline depth are determined using lake-specific hypsography. The
274 criteria for stratification include a vertical density gradient between the surface and bottom
275 layer of at least 0.05 kg m^{-3}, an average water column temperature above 4 °C, and the
276 presence of a derived thermocline (Ladwig et al. 2021). For any day that does not meet all of
277 these criteria, the water column is considered to be fully mixed. The thermocline depth
278 values are smoothed using a moving average with a window size of 14 days to prevent large
279 entrainment fluxes that can destabilize the model at very short time scales when thermal
280 strata are shallow. During mixed periods, the entire lake is treated as the epilimnion, and a
281 separate hypolimnion is not incorporated into the model dynamics. Ice cover in the model is
282 determined using the "ice flag" provided in the derived temperature profile data from Read et
283 al. (2021). Our metabolism model does simulate under-ice conditions, however we do not
284 include the presence of inverse stratification during winter periods.

2.3.2 External Lake and Environment Physical Fluxes

Atmospheric exchange of DO, external loading of OC, and outflow of OC are the three environmental boundary fluxes accounted for in the water quality model (Table 2 Eq. 9-11). The gas exchange velocity for atmospheric exchange is determined using the Cole and Caraco model (1998) and is calculated using the LakeMetabolizer R package (Winslow et al. 2016). Oxygen saturation values are also calculated using this package. During ice covered conditions, we assume that the atmospheric exchange value is ten percent of the value during non-ice covered conditions based on sea ice gas exchange estimates (Loose and Schlosser, 2011).

For the northern lakes (TR, AL, BM, SP), we assume that allochthonous OC loads consist of entirely recalcitrant substrates. We verify total OC load, total inflow concentration, and recalcitrant OC export values with estimates from Hanson et al. (2014). For ME, we verify the total annual allochthonous OC load and OC inflow concentrations against observed inflow data from Hart et al. (2017) by back calculating inflow concentrations based on the modeled OC equilibrium of the lake. MO inflow concentrations are equivalent to the in-lake epilimnetic concentrations of OC from ME at each model time step. The total OC loads for MO are verified based on the total allochthonous load found in McCullough et al. 2018.

Table 2. Equations for the model, organized by state variables, [*DO* (dissolved oxygen), *DOCL* (labile dissolved organic carbon), *DOCR*(recalcitrant dissolved organic carbon), *POCL* (labile particulate organic carbon), *POCR* (recalcitrant particulate organic carbon), *Secchi*] and relevant fluxes. *Note:* The entrainment flux (*Entr*) is only included during thermally stratified periods. The inflow (*IN*) and outflow (*OUT*) fluxes are not included in

the calculations for the hypolimnetic layer. The inflow of labile DOC (IN_{DOCL}) parameter in Eq. 2 is only used for calculating allochthonous OC loads for MO. Atmospheric gas exchange of dissolved oxygen ($AtmExch$) is not included for the hypolimnetic DO calculation. Normalized total phosphorus is represented by (TP_{norm}). The volume (V) term represents the respective lake layer volume, or the discharge volume for the inflow and outflow equations. The term (r_{rate}) is included in Eq. 13 to represent the respiration rates of the different OC pools. It is included to simplify the table of equations. Terms not defined here are included in Table 3.

State Variables	
DO [gDO] $\frac{dDO}{dt} = (NPP * O2_{convert}) + AtmExch + Entr_{DO} - (R_{sed} * O2_{convert}) - (R_{wc} * O2_{convert})$	(1)
DOCL [gC] $\frac{dDOC_L}{dt} = (NPP * (1 - C_{NPP})) + IN_{DOCL} + Entr_{DOCL} - R_{DOCL} - OUT_{DOCL}$	(2)
DOCR [gC] $\frac{dDOC_R}{dt} = IN_{DOCR} + Entr_{DOCR} - OUT_{DOCR} - R_{DOCR\,Epi}$	(3)
POCL [gC] **Mixed and Epi:** $\frac{dPOC_L}{dt} = (NPP_{Epi} * C_{NPP}) + IN_{POCL} + Entr_{POCL} - R_{POCL\,Epi} - Settle_{POCL\,Epi} - OUT_{POCL}$ **Hypo:** $\frac{dPOC_L}{dt} = (NPP_{Hypo} * C_{NPP}) + Settle_{POCL\,Epi} - Settle_{POCL\,Hypo} - R_{POCL\,Hypo} - Ent_{POCL}$	(4) (5)
POCR [gC] **Mixed and Epi:** $\frac{dPOC_R}{dt} = IN_{POCR} + Entr_{POCR} - OUT_{POCR} - R_{POCR\,Epi} - Settle_{POCR\,Epi}$ **Hypo:** $\frac{dPOC_R}{dt} = Settle_{POCR\,Epi} - Settle_{POCR\,Hypo} - R_{POCR\,Hypo} - Entr_{POCR}$	(6) (7)
Secchi [m] $Secchi = \frac{1.7}{K_{LEC}}$	(8)
Fluxes	
Atm exchange [gDO d^{-1}] $AtmExch = K_{DO} * (DO_{sat} - DO_{prediction}) * Area_{sfc}$	(9)
Inflow [gC d^{-1}] $IN = Carbon\ Concentration_{inflow} * V_{inflow}$	(10)
Outflow [gC d^{-1}] $OUT = Carbon\ Concentration_{outflow} * V_{outflow}$	(11)
Net Primary Productivity [gC d^{-1}] $NPP = Pmax * (1 - e^{(-IP * \frac{Light}{Pmax})}) * TP_{norm} * \theta_{NPP}{}^{(T-20)} * V$	(12)
Respiration [gC d^{-1}] $R_{wc} = Carbon\ Pool * r_{rate} * \theta_{Resp}{}^{(T-20)} * \frac{DO\ Concentration}{DO_{1/2} + DO\ Concentration}$	(13)
Sediment Respiration [gC d^{-1}] $R_{sed} = r_{sed} * \theta_{Resp}{}^{(T-20)} * \frac{DO\ Concentration}{DO_{1/2} + DO\ Concentration} * Area_{sed}$	(14)
POC settle [gC d^{-1}] $Settle = (POC\ Pool * K_{POC}) * \frac{Area}{V}$	(15)

Entrainment [gC d^{-1}]

$$V_{Entr} = V_{epi}(t) - V_{epi}(t-1) \quad (16)$$

$V_{Entr} > 0$ (Epilimnion growing)

$$Entr = \frac{V_{Entr}}{V_{Hypo}} * Carbon\ Pool_{Hypo} \quad (17)$$

$V_{Entr} < 0$ (Epilimnion shrinking)

$$Entr = \frac{V_{Entr}}{V_{Epi}} * Carbon\ Pool_{Epi} \quad (18)$$

Light [W m^{-2}]

$$Light = \int_{z_1}^{z_2} (I_{z_1} * e^{-(K_{LEC} * z)})\, dz * (1-\alpha) \quad (19)$$

Light Extinction Coefficient [Unitless]

$$K_{LEC} = LEC_{water} + (LEC_{POC} * ((\frac{POCL}{V}) + (\frac{POCR}{V}))) + (LEC_{DOC} * ((\frac{DOCL}{V}) + (\frac{DOCR}{V}))) \quad (20)$$

2.3.3 Internal Lake Physical Fluxes

The two in-lake physical fluxes included in the model are POC settling and entrainment of all state variables. POC settling is the product of a sinking rate (m d^{-1}) and the respective POC pool (g), divided by the layer depth (m) (Table 2 Eq. 15). Sinking rates are either borrowed from literature values (Table 3) or fit during model calibration (see below). Entrainment is calculated as a proportion of epilimnetic volume change (Table 2 Eq. 17-18). A decrease in epilimnetic volume shifts mass of state variables from the epilimnion into the hypolimnion, and an increase in volume shifts mass from the hypolimnion to the epilimnion.

2.3.4 Internal Lake Metabolism Fluxes

The metabolism fluxes in the model are net primary production (NPP) and respiration (R). Respiration includes water column respiration for each OC state variable in the epilimnion and hypolimnion and is calculated at each time step as the product of the OC state variable and its associated first order decay rate (Table 2, Eq. 13). Sediment respiration for the hypolimnion during stratified periods and the epilimnion (entire lake) during mixed periods is a constant daily rate that is individually fit for each lake. Note that we did not include

337 anaerobic carbon metabolism in our modeling approach and discuss potential shortcomings
338 in the discussion section. We assume inorganic carbon is not a limiting carbon source. In the
339 model, we consider any DO concentration less than 1 g DO m^{-3} to be anoxic (Nürnberg
340 1995).
341
342 NPP is tracked in both the epilimnion and hypolimnion. NPP is a function of light, total
343 phosphorus concentration, temperature, a maximum productivity coefficient (*Pmax*), and a
344 slope parameter defining the irradiance and productivity curve (*IP*) (Table 2 Eq. 12). Total
345 phosphorus concentration in a layer is taken from observational data for each lake
346 interpolated to the daily time scale. Maximum daily primary production rates were taken
347 from Wetzel (2001). As these maximum production rates are not phosphorus-specific but
348 subsume lake-specific nutrient concentrations, we multiplied them with time-transient,
349 normalized TP concentrations. Normalizing was done by removing the mean of observed TP
350 and dividing by TP variance. This allows us to retain the time dynamics of the normalized
351 TP, which we use to represent seasonal TP dynamics for each lake. The Arrhenius equation
352 provides temperature control for NPP, and we determined through model fitting a θ of 1.12.
353 All OC derived from NPP is assumed to be labile and is split between particulate and
354 dissolved OC production, with eighty percent produced as POC and twenty percent produced
355 as DOC. This ratio was determined through model fitting and is similar to previously
356 reported values (Hipsey et al. 2022). Average light in a layer is calculated for each day and is
357 dependent on the depth of a layer and the light extinction coefficient (Table 2 Eq. 19). During

358 ice covered conditions, average light is assumed to be five percent of the average non-ice
359 covered value (Lei et al. 2011).
360
361 Epilimnetic and hypolimnetic water column respiration is tracked independently for each OC
362 pool in the model. During mixed periods, there are four OC pools – DOCR, DOCL, POCR,
363 POCL. During stratified periods, those pools are split into a total of eight pools that are
364 tracked independently for the epilimnion and hypolimnion. Respiration is calculated as a
365 product of the mass of a respective variable, a first order decay rate coefficient, temperature,
366 and oxygen availability (Table 2 Eq. 13). The respiration decay rate coefficients are based on
367 literature values (Table 3) or were fit during model calibration. An Arrhenius equation is
368 used for temperature control of respiration, with θ_{Resp} equal to 1.04, which was determined
369 through manual model fitting. The respiration fluxes are also scaled by oxygen availability
370 using the Michaelis-Menten equation with a half saturation coefficient of 0.5 g DO m^{-3}, such
371 that at very low DO concentrations, the respiration flux approaches zero.
372
373 Sediment respiration is calculated from a constant daily respiration flux, adjusted for
374 temperature and oxygen availability, using the Arrhenius and Michaelis-Menten equations,
375 respectively (Table 2 Eq. 14). The mass of sediment OC is not tracked in the model. During
376 stratified periods, we assume that the majority of epilimnetic sediment area is in the photic
377 zone, and therefore has associated productivity from macrophytes and other biomass. It is
378 assumed that this background productivity and sediment respiration are of similar magnitude
379 and inseparable from water column metabolism, given the observational data. Therefore,

epilimnetic sediment respiration is not accounted for in the model during stratified conditions. During mixed conditions, we assume that sediment respiration is active on all lake sediment surfaces, which are assumed to be equivalent in area to the total surface lake area. During stratified periods, we use the area at the thermocline as the sediment area for calculating hypolimnetic sediment respiration.

2.3.5 Other in-lake calculations and assumptions

We calculate a total light extinction coefficient (LEC) for the epilimnion and hypolimnion. The total LEC for each layer is calculated by multiplying the dissolved and particulate specific LEC values with their respective OC state variable concentrations, combined with a general LEC value for water (Table 2 Eq. 20). This total LEC value is used to calculate a daily estimate of Secchi depth (Table 2 Eq. 8). The coefficients for the light extinction of water, DOC, and POC are manually calibrated based on observed Secchi depth ranges for the study lakes (Table 3, SI Table 5).

Table 3. Model Parameters, grouped into three categories: constants, which are values that were not tuned; manually calibrated, which are parameters manually tuned, typically guided by ranges from the literature; and parameters calibrated through constrained parameter search, which are calibrated through an automated search of parameter space.

Parameter	Abbreviation	Value	Units	Source
Constants				
Conversion of Carbon to Oxygen	$O2_{convert}$	2.67	Unitless	Mass Ratio of C:O
Respiration rate of DOCR	r_{DOCR}	0.001	day^{-1}	(Hanson et al., 2011)

Parameter	Abbreviation	Value	Units	Source
Respiration rate of POCR	r_{POCR}	0.005	day^{-1}	Taken from ranges provided in (Hanson et al. 2004)
Respiration rate of POCL	r_{POCL}	0.2	day^{-1}	Taken from ranges provided in (Hipsey et al. 2022)
Michaelis-Menten DO half saturation coefficient	$DO_{1/2}$	0.5	$g\ \ m^{-3}$	Taken from ranges provided in (Hipsey et al. 2022)
Light extinction coefficent of water	LEC_{water}	0.125	m^{-1}	Taken from ranges in Hart et al. (2017)
Ratio of DOC to POC production from NPP	C_{NPP}	0.8	Unitless	Biddanda & Benner (1997)
Albedo	α	0.3	Unitless	Global average (Marshall & Plumb, 2008)
Atmospheric gas exchange adjustment during ice covered conditions	C_{winter}	0.1	Unitless	Taken from ranges in (Loose & Schlosser, 2011)
Coefficient of light transmitted through ice	C_{ice}	0.05	Unitless	Taken from ranges provided in (Lei et al. 2011)
Settling velocity rate of POC_R	K_{POCR}	1.2	$m\ \ day^{-1}$	Taken from ranges found in (Reynolds et al.1987)
Settling velocity rate of POC_L	K_{POCL}	1	$m\ \ day^{-1}$	Taken from ranges ranges found in (Reynolds et al.1987)
Temperature scaling coefficient for NPP	θ_{NPP}	1.12	Unitless	Taken from values provided in (Hipsey et al. 2022) and (Ladwig et al. 2021)
Temperature scaling coefficient for Respiration	θ_{Resp}	1.04	Unitless	Taken from values provided in (Hipsey et al. 2022) and (Ladwig et al. 2021)
Manually calibrated				

Parameter	Abbreviation	Value	Units	Source
Light extinction of DOC	LEC_{DOC}	0.02 - 0.06	$m^2 g^{-1}$	Manually calibrated based on observed Secchi Depth ranges for the study lakes
Light extinction of POC	LEC_{POC}	0.7	$m^2 g^{-1}$	Manually calibrated based on observed Secchi Depth ranges for the study lakes
Maximum Daily Productivity	$Pmax$	0.5-5	$g\ \ m^{-3} day^{-1}$	Manually calibrated from mean productivity values from Wetzel (2001)
Recalcitrant DOC inflow concentration	$DOCR_{inflow}$	5-10	$g\ \ m^{-3}$	Based on ranges found in (Hanson et al. 2014, McCullough et al. 2018, Hart et al. 2017)
Recalcitrant POC inflow concentration	$POCR_{inflow}$	2-5	$g\ \ m^{-3}$	Based on ranges found in (Hanson et al. 2014, McCullough et al. 2018, Hart et al. 2017)
Calibrated through constrained parameter search				
Slope of the irradiance/productivity curve	IP	0.045, 0.015	$gCd^{-1}(Wm^{-2})^{-1}$	Based on ranges found in (Platt et al. 1980) and tuned separately for each lake region (South, North)
Sediment respiration flux	r_{SED}	0.05 – 0.4	$g\ \ m^{-2} day^{-1}$	Based on ranges found in (Ladwig et al. 2021) and (Mi et al. 2020) and fit independently for each lake
Respiration rate of DOCL	r_{DOCL}	0.015 - 0.025	day^{-1}	Based on ranges found in (McCullough et al. 2018) and fit for each lake independently

2.4 Model Sensitivity and Parameter Calibration

To better understand the sensitivities of the model output to parameter values, we performed a sensitivity analysis of the model parameters using the global sensitivity method from

Morris (1991). The sensitivity analysis showed that there were nine parameters to which the model was consistently sensitive across the six study lakes. This group included the ratio of DOC to POC produced from NPP (C_{NPP}), the maximum daily productivity parameter (*Pmax*), the inflow concentration of recalcitrant POC ($POCR_{inflow}$), the setting velocity of recalcitrant POC (K_{POCR}), the temperature fitting coefficients for productivity and respiration (θ_{NPP}, θ_{Resp}) the slope of the irradiance/productivity curve (*IP*), the sediment respiration flux (r_{SED}), and the respiration rate of DOCL (r_{DOCL}). We chose a subset of the nine parameters to include in the uncertainty analysis based on the following justifications. The model results showed that recalcitrant substrates are of lesser importance for lake metabolism dynamics, so we chose not to further investigate the uncertainty of the $POCR_{inflow}$ and K_{POCR} parameters. The *Pmax* and *IP* parameters are directly correlated, so we chose to remove Pmax from further uncertainty considerations. The θ_{NPP} and θ_{RESP} parameters act as substitutes for water temperature, a well-known "master variable" in water quality modeling, and directly reflect seasonality in the model. Therefore, we chose to omit these parameters for further uncertainty calculations. The final subset of parameters for uncertainty analysis consisted of C_{NPP}, r_{DOCL}, r_{SED}, and *IP*. Of the four parameters, we felt C_{NPP} was best constrained by the literature. To reduce the number of parameters estimated in the calibration process we restricted the automated constrained parameter search to the remaining three.

Model parameters are grouped into three categories: constants, manually calibrated, and parameters calibrated through an automated constrained parameter search. The constant parameters are consistent across the study lakes and are not tuned. The manually calibrated parameters were allowed to vary by lake and are typically guided by ranges from the

literature. The constrained parameter search uses an automated search of parameter space, constrained by literature values, to fit the *IP*, r_{SED}, and r_{DOCL} parameters for the study lakes. Specifically, we performed a constrained fitting of the model to observational data using the Levenberg-Marquardt algorithm within the "modFit" function of the "FME" R package (Soetaert & Petzoldt, 2010). During the model fitting, errors in modeled DO, DOC, and Secchi depth are weighted equally in the southern lakes. Secchi depths in the northern lakes were highly stochastic, and therefore we use a moving average on observational data and predictions of Secchi depth and calculate the residuals as the difference between the two averaged time series. We use a moving average window of 15 observations because we want to capture the average annual Secchi depth trend, and there are roughly 15 observations per year.

The first 15 years of the model output was used for calibration and the last 5 years were used for model validation. We chose the first 15 years for calibration because the observational data were relatively stable and were not indicative of any large trends in ecosystem processes, as opposed to the last five years which showed slightly more model deviation from DOC observational data in the southern lakes (SI Fig. 2).

2.5 Model Uncertainty

Sensitivity guided the uncertainty analysis. To quantify uncertainty around model predictions, we sampled *IP*, r_{SED}, and r_{DOCL} simultaneously from uniform distributions defined by +-30% of the literature ranges used for our calibrated parameter values (Table 3). We ran one hundred model iterations randomly sampling the three model state variables

450 across these distributions. We plotted the minimum and maximum values for these uniform
451 distributions and included them in the time series plots (Fig. 2, 3, 4, SI Fig. 1,2,3).
452
453 **3 Results**
454
455 **3.1 Model Fit to Ecosystem States**
456 Model predictions of DO reproduce observed seasonal variability well. Note that RMSE
457 values presented here represent model error combined over both the validation and
458 calibration periods (see Supplementary Material: Table S1 for calibration and validation
459 specific RMSE values), and that state variables are presented with truncated time ranges for
460 visual clarity (see Supplementary Material: Fig. S1-S3 for full time series). Epilimnetic DO
461 generally has lower RMSE than DO in the hypolimnion (Fig. 2). In the epilimnion, RMSE
462 ranges from 0.74 g DO m^{-3} (TR) to 2.11 g DO m^{-3} (MO), and in the hypolimnion, RMSE
463 ranges from 1.22 g DO m^{-3} (ME) to 2.77 g DO m^{-3} (AL, SP). Validation NSE values for DO
464 ranged from -1.45 (AL) to 0.02 (ME) in the epilimnion and -0.30 (SP) to 0.86 (ME) in the
465 hypolimnion. Validation KGE values for DO ranged from 0.40 (AL) to 0.90 (TR) in the
466 epilimnion and 0.35 (SP) to 0.80 (ME) in the hypolimnion. KGE and NSE values for all
467 lakes can be found in SI Table 7. In the southern lakes, modeled values reach anoxic levels
468 and generally follow the DO patterns recorded in the observed data (Fig. 2a-b).
469 Observational data for the northern lakes show an occasional late summer onset of anoxia,
470 and these events are generally captured in the model output. A late summer spike in
471 hypolimnetic DO predictions commonly occurs as well, which is likely a model artifact
472 caused by the reduction of hypolimnetic volumes to very small values over short time periods

prior to fall mixing. Reduction to small volumes, coincident with modest fluxes due to high concentration gradients, result in transient high concentrations. Overall, the goodness-of-fit of hypolimnetic DO in our study lakes does not seem to follow any regional or lake characteristic patterns.

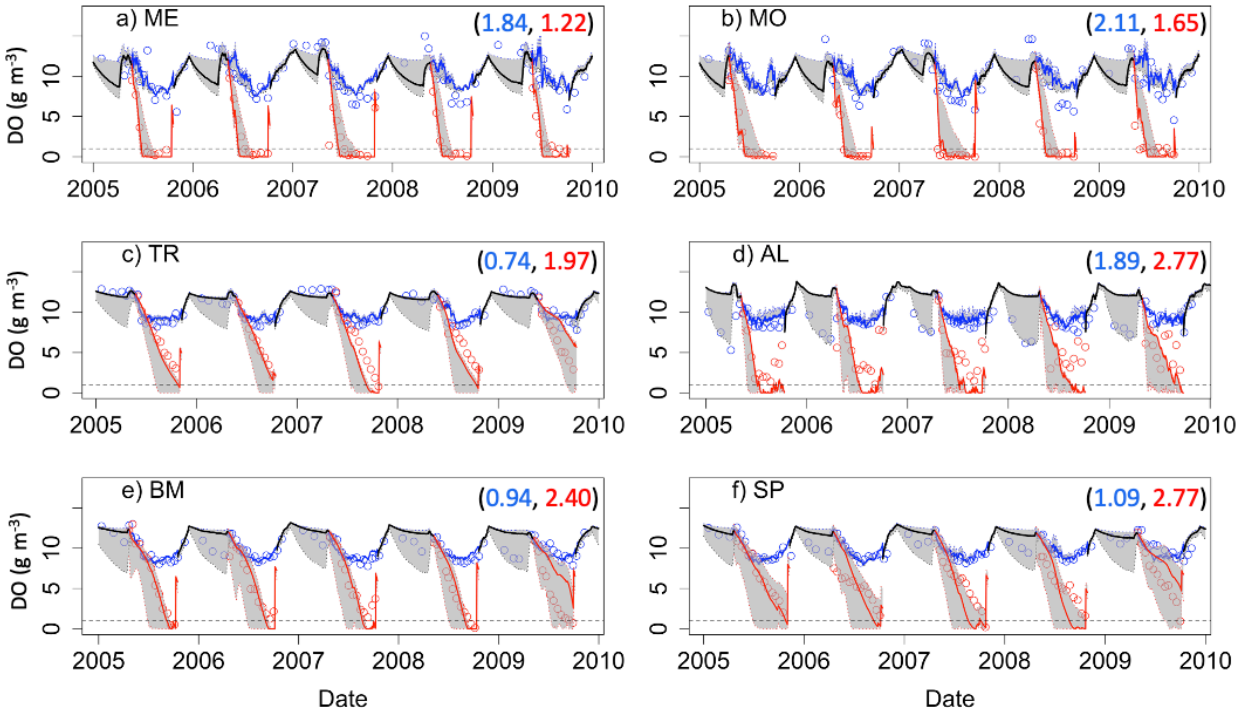

Figure 2. Dissolved oxygen (DO) time series for the years, 2005-2010, for the six study lakes (a-f). Model predictions are represented by lines, and circles represent the observational data. Epilimnetic DO values are blue and Hypolimnetic DO values are red. Fully mixed periods for the lake are indicated by a single black line. RMSE values (epilimnion, hypolimnion; g m^{-3}) for the validation period are included in the upper right of each panel. Uncertainty is represented by gray shading.

The two southern lakes (ME, MO) have epilimnetic DOC RMSE values greater than 1.00 g C m^{-3}, while the RMSE for northern lakes ranges from 0.41 g C m^{-3} (TR) to 0.70 g C m^{-3} (AL) (Fig. 3). In the southern lakes, NSE epilimnetic DOC values were below -3.00 and KGE values ranged from -0.29 to -0.32. In the northern lakes, NSE values for DOC ranged

between -2.75 (SP) and -0.31 (AL). KGE values ranged from -0.07 (BM) to 0.35 (TR). All NSE and KGE metrics for DOC can be found in SI Table 7. Observational data in both southern lakes indicate a decrease in DOC concentration beginning around 2010, which is largely missed in the model predictions (Fig.3a-b, Supplementary Material: Fig. S2a-b) and cause an overestimation of DOC by about 1-2 g C m^{-3}. However, model predictions converge with observed DOC toward the end of the study period (Supplementary Material: Fig. S2a-b). In AL, the seasonal patterns of modeled DOC are smaller in amplitude than the observational data (Supplementary Material: Fig. S2d).

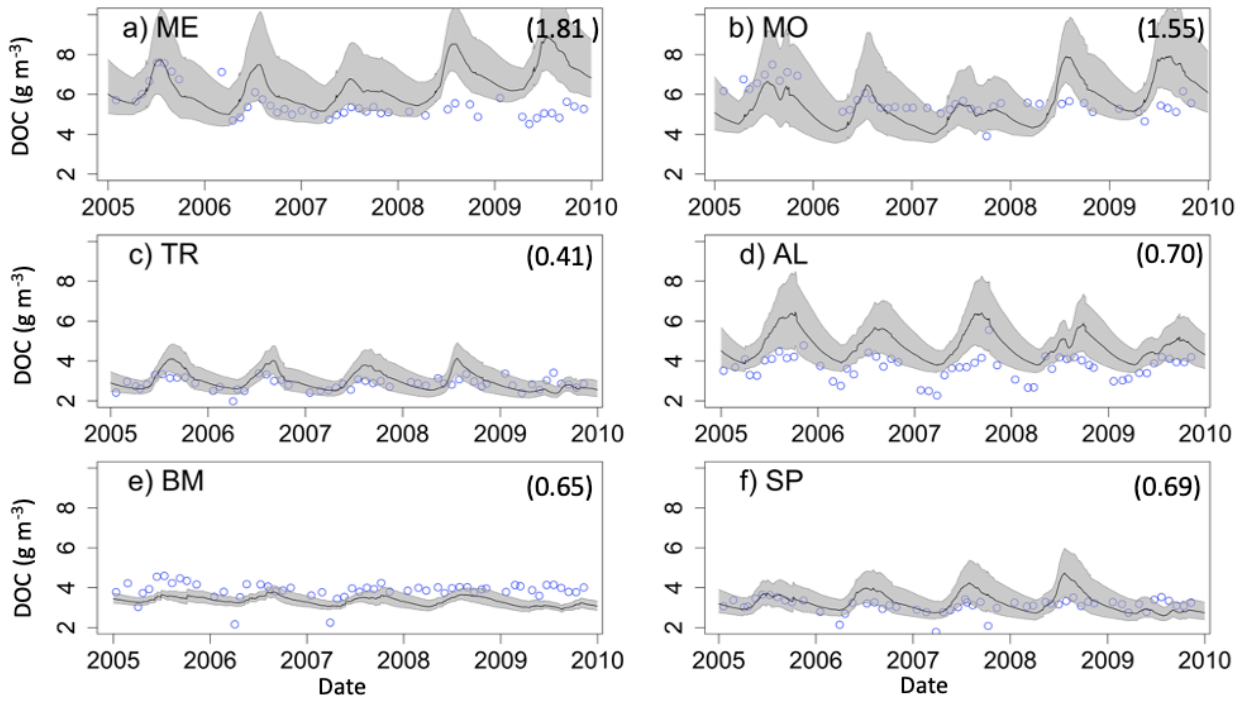

Figure 3. Epilimnetic dissolved organic carbon (DOC) time series for the years, 2005-2010, for the six study lakes (a-f). Model predictions are represented by lines, and circles represent the observational data. RMSE values for the validation period are included for each lake (g C m^{-3}). Uncertainty is represented by gray shading.

Secchi depth predictions reproduce the mean and seasonal patterns in all lakes (Fig. 4). Although the model produced annual cycles of Secchi depth that generally covered the range of observed values, short term deviations from annual patterns in the observed data are not reproduced. The timing of minima and maxima Secchi depth sometimes differed between predicted and observed values for the northern lakes. In addition, winter extremes in observed Secchi depth are not always reproduced by the model, which is especially evident for ME (Fig. 4a). However, winter observational data for Secchi are more sparse than other seasons.

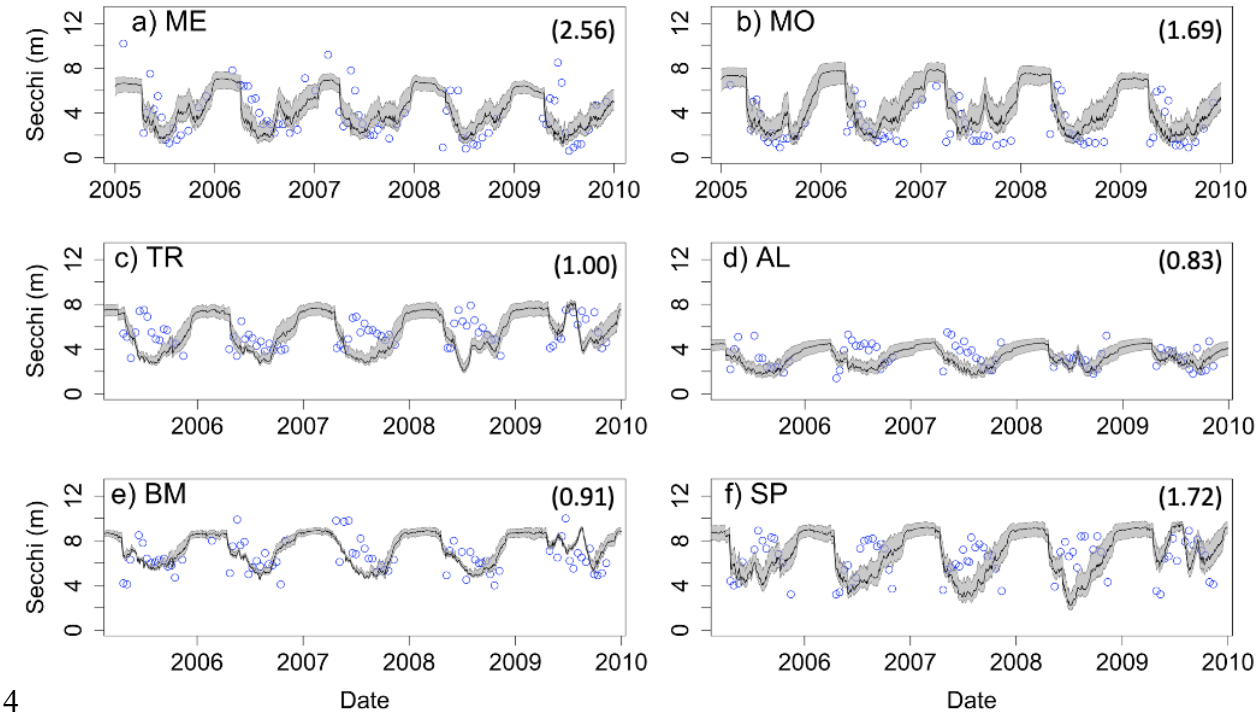

Figure 4. Secchi depth time series for the years, 2005-2010, for the six study lakes (a-f). Model predictions are represented by lines, and circles represent the observational data. RMSE values for the validation period are included for each lake (m). Uncertainty is represented by gray shading.

3.2 Ecosystem Processes

The mean annual OC budgets of all six lakes show large differences in the sources and fates of OC among lakes (Fig. 5; Supplementary Material: Table S3). Autochthony is the dominant source of OC for all study lakes. Water column respiration is the largest portion of whole-lake respiration in ME, MO, TR, SP, and BM. Sediment respiration contributions are a lower proportion of total respiration in ME, MO, and TR (mean of 14.1%), and are slightly higher in BM and SP (mean of 18.7%). AL has a more even distribution of OC fates. OC burial amounts also vary across the study lakes, with the highest percentage in AL (34.1%), and lowest in SP (5.25%).

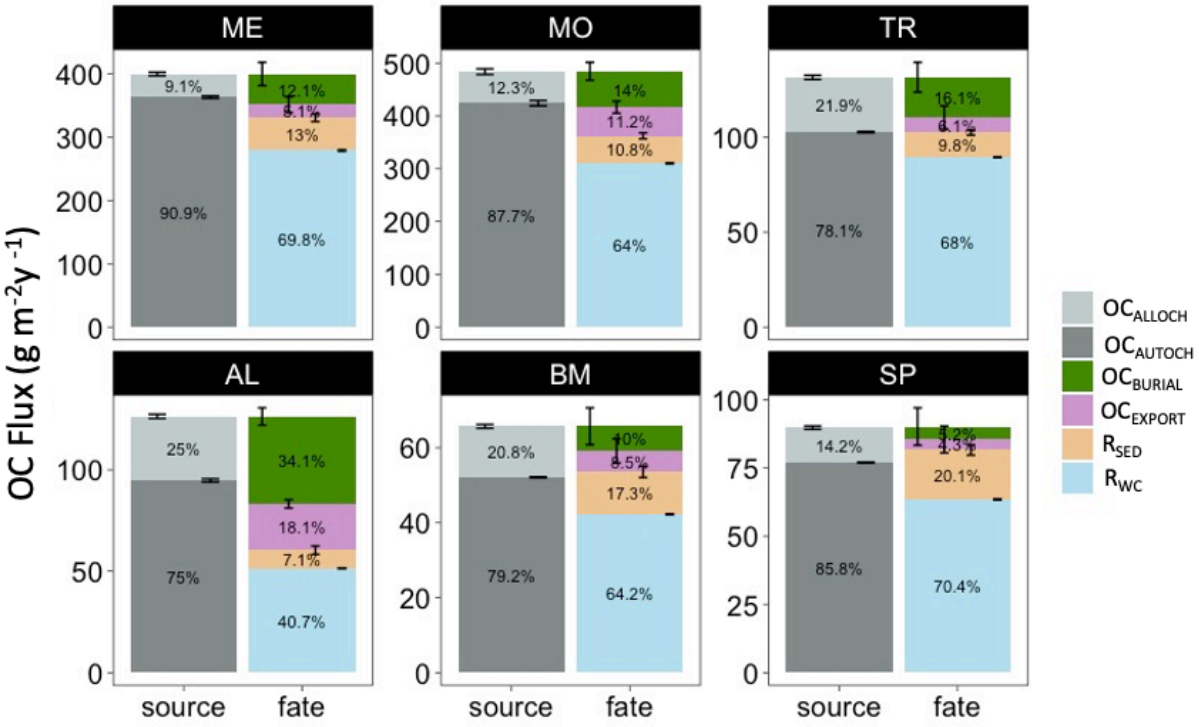

Figure 5. Total annual budget, sources (left stacked bars) and fates (right stacked bars), of organic carbon (OC) in each lake over the study period. The OC sources include allochthonous OC (OC_{ALLOCH}) and autochthonous OC (OC_{AUTOCH}). The OC fates include burial of OC (OC_{BURIAL}), export of OC (OC_{EXPORT}), sediment respiration of OC (R_{SED}), and water column respiration of OC (R_{WC}). Standard error bars for the annual means are indicated for each source and fate as well. Note that the magnitudes of the y-axis differ

among the lakes. A significance test comparing these fluxes across the study lakes can be found in SI Table 6.

The lakes show inter-annual variation in trophic state, as quantified by NEP (Fig. 6). Total respiration (water column and sediment) exceeds autochthony in SP, BM, and TR, indicating predominantly net heterotrophy for these systems. The remaining lakes (ME, MO, AL) are generally net autotrophic. The southern lakes (ME, MO) are net autotrophic (positive NEP) for the majority of the study years but became less autotrophic over the last five years of the study period (2010-2014). BM and SP are mostly net heterotrophic (negative NEP) over the study period with a few brief instances of net autotrophy. The strongest autotrophic signal for these lakes occurred around 2010. TR experienced prolonged periods of both autotrophy and heterotrophy. AL is net autotrophic over the study period but had lower average NEP than the southern lakes. ME, MO, and AL all have negative trends in NPP, but only ME and AL were significant ($p\_value < 0.1$, Mann-Kendall test) (SI Table 2). Of these three lakes, ME and AL also have decreasing significant trends in annual total phosphorus concentration (SI Table 2). No significant trends were found for NPP or total phosphorus in the other lakes (MO, TR, BM, SP). It is worth noting that our interpretation of metabolism dynamics in the results are based on the median NPP and Respiration flux values produced by the model. Because of the high uncertainty associated with these fluxes, we should be cautious about asserting inferences about long term changes in trophic state.

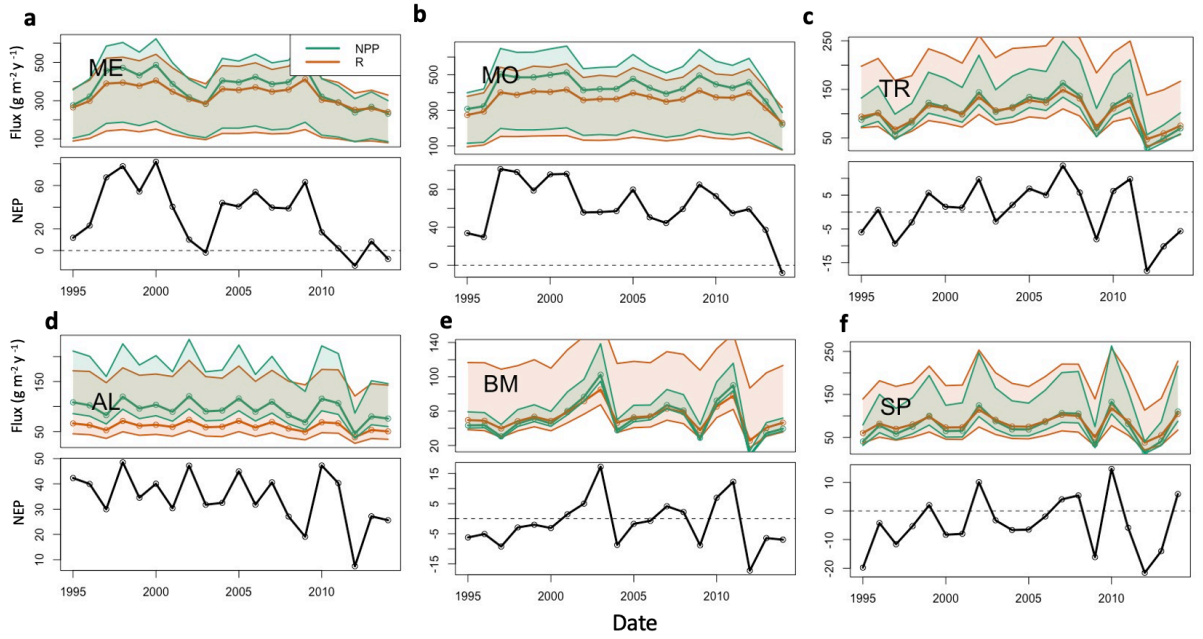

Figure 6. Time series of calibrated lake Net Primary Production (green), Total Respiration (red) (top panels), and Net Ecosystem Production (NEP, bottom panels) for the six lakes: (a) Lake Mendota; (b) Lake Monona; (c) Trout Lake; (d) Allequash Lake; (e) Big Muskellunge Lake, and; (f) Sparkling Lake. Fluxes are in units of $gC\ m^{-2}y^{-1}$. Solid line represents prediction based on best parameter estimates. Shaded regions represent prediction uncertainty based on parameter ranges in Table 3. Shaded region for NEP not shown to reduce axis limits and emphasize NEP pattern.

Hypolimnetic DO consumption during stratified periods was modeled as a function of the two components of hypolimnetic respiration, hypolimnetic water column respiration and hypolimnetic sediment respiration. Water column respiration contributes more than sediment respiration to total hypolimnetic respiration in the deepest lakes. In ME and MO, the mass of summer autochthonous POC entering the hypolimnion is similar to the total hypolimnetic OC mass respired for the beginning of the stratified period (Fig. 7a-b; green line). Later in the stratified period, an increase in epilimnetic POC and associated settling exceeds total hypolimnetic respiration (Fig. 7a-b; green hashed area). This is due, in part, to lower respiration rates that occur once DO (gray line) has been fully depleted, which occurs in early

July for ME and late June for MO. In BM and SP the total hypolimnetic respiration slightly exceeds autochthonous POC inputs during parts of the stratified period, indicating the importance of allochthony in these systems (Fig. 7c,f). BM shows that autochthonous POC entering the hypolimnion and total hypolimnetic respiration are similar for much of the stratified period (Fig. 7d). AL is the only lake to have autochthonous POC inputs consistently larger than total hypolimnetic respiration during the stratified season. All lakes show that summer allochthonous POC entering the hypolimnion is a small contribution to the overall hypolimnetic POC load.

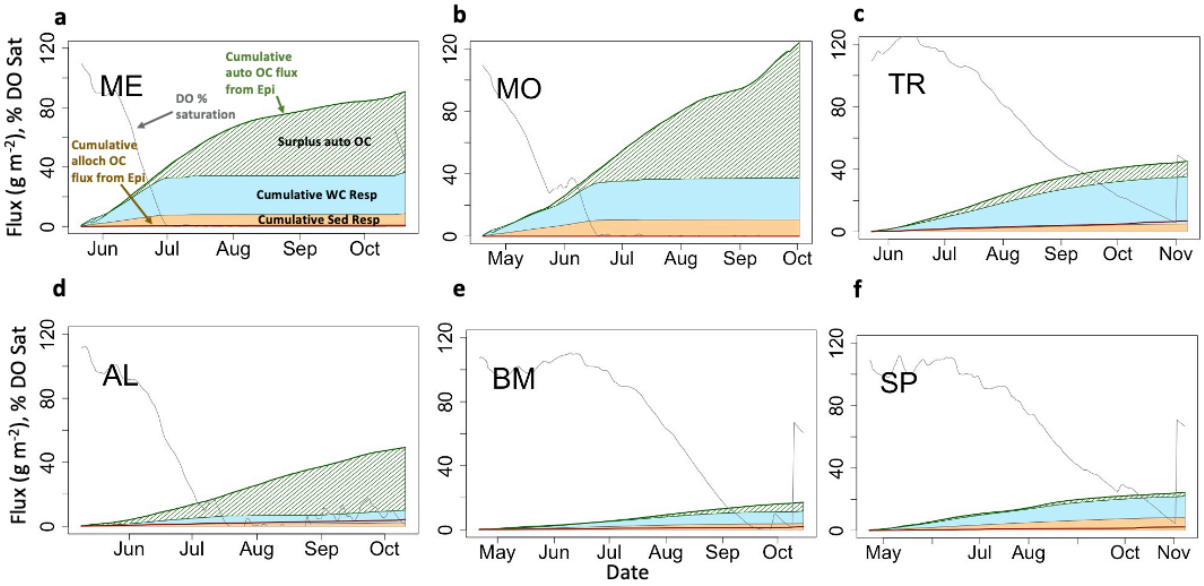

Figure 7. Hypolimnetic dissolved oxygen, allochthonous (alloch) and autochthonous (auto) organic carbon loading, and respiration dynamics during one stratified period (2005) for each lake. Fluxes are cumulative $gC\ m^{-2}$ and DO is presented as percent saturation. Labels are in panel (a). Note that the cumulative water column (WC) and sediment (Sed) respiration fluxes are stacked, while other cumulative fluxes are not.

Respiration of autochthonous POC and sediment respiration account for most of the total hypolimnetic respiration in all lakes (Fig. 8). Respiration of DOC accounts for a relatively

small proportion of total respiration. Total hypolimnetic respiration is higher in the southern lakes than the northern lakes. TR has the highest amount of hypolimnetic respiration for the northern lakes, and AL and BM have the least amounts of hypolimnetic respiration. Water column respiration contributed the most towards total hypolimnetic respiration in all lakes. Sediment respiration contributed the largest proportion towards total hypolimnetic respiration in BM and SP. DOC water column respiration was the smallest proportion of total hypolimnetic respiration in all six study lakes.

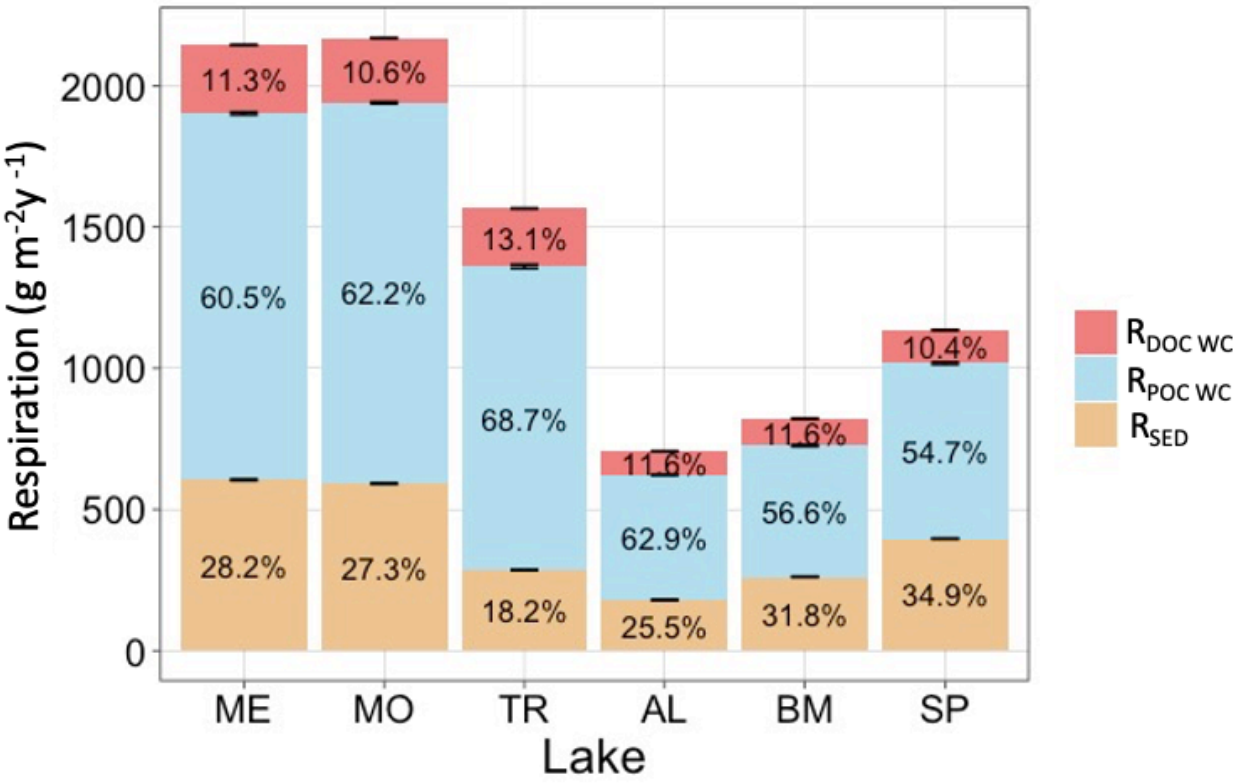

Figure 8. Total average annual hypolimnetic respiration, separated by percentages attributed to water column DOC ($R_{DOC\ WC}$), water column POC ($R_{POC\ WC}$), and sediment (R_{SED}) organic carbon sources. Standard error bars for the annual respiration values are indicated as well.

4 Discussion

4.1 Autochthonous and Allochthonous Loads

Autochthony was the dominant source of OC subsidizing hypolimnetic respiration in the modeling results for our study lakes. The high contribution of autochthonous OC to ecosystem respiration, relative to that of the allochthonous pool, was surprising, given ample research highlighting the dominance of allochthonous OC in north temperate lakes (Wilkinson et al. 2013; Hanson et al. 2011; Hanson et al. 2014). Similar to what was found by Wilkinson et al (2013), the standing stock of DOC in the water column of lakes in our study was from predominantly allochthonous sources. However, we emphasize in our study that autochthonous OC pools have higher turnover rates than allochthonous OC pools (Dordoni et al., 2022) and often are lower in concentration than the more recalcitrant allochthonous pools (Wilkinson et al. 2013). Thus, studies based on correlative relationships between lake concentrations of organic matter and water quality metrics, likely overlook the importance of more labile organic matter in driving observable ecosystem phenomena, such as gas flux and formation of hypolimnetic anoxia (Evans et al., 2005; Feng et al., 2022). By quantifying metabolism fluxes relevant to both OC pools, we can recreate shorter-term OC processes that quantify high turnover of labile organic matter, which would typically be missed by empirical studies based on monthly or annual observations.

Allochthony and autochthony are important to lake carbon cycling, but in ways that play out at different time scales. Allochthonous OC has been well-established as an important factor in driving negative NEP through a number of mechanisms (Wilkinson et al., 2013; Hanson et al., 2014; Hanson et al., 2011). Allochthony contributes to water quality variables, such as

Secchi depth (Solomon et al. 2015), by providing the bulk of DOC in most lakes (Wilkinson et al., 2013) and can drive persistent hypolimnetic anoxia in dystrophic lakes (Knoll et al., 2018). In contrast, autochthony contributes to seasonal dynamics of water quality through rapid changes in OC that can appear and disappear within a season. Within that seasonal time frame, autochthonous POC settling from the epilimnion can drive hypolimnetic respiration, thus controlling another key water quality metric, oxygen depletion. It is worth noting that our model does not discern allochthonous and autochthonous sediment OC, however we show that autochthonous OC makes up the largest proportion of OC loads in our study lakes and therefore autochthony likely contributes substantially to the sediment OC pool. For highly eutrophic lakes, the model results show excess autochthony stored in the sediments which may carry into subsequent years, potentially providing additional substrate for sediment respiration. Thus, understanding and predicting controls over hypolimnetic oxygen depletion benefits from quantifying both allochthonous and autochthonous OC cycles.

Differences in trophic status, hydrologic residence time, and inflow sources help explain the relative proportion of allochthonous versus autochthonous OC among lakes in our study. Water residence times (Hotchkiss et al. 2018; McCullough et al. 2018) and surrounding land cover (Hanson et al. 2014) have been shown to have a substantial impact on OC dynamics by controlling allochthonous OC loading and NEP trends on lakes included in our study (Hanson et al. 2014, McCullough et al. 2018). We built upon these ideas by recreating daily watershed loading dynamics of POC and DOC from derived discharge data and incorporating nutrient control over lake primary production by using high quality and long-term

observational data. The northern lakes are embedded in a forest and wetland landscape, which are characteristic of having higher DOC than the urban and agricultural landscape of the southern lakes (Creed et al., 2003). This creates variation in allochthonous loading across the study lakes. Lake trophic state and productivity are a major control for autochthonous production, which influences autochthonous loads across the study lakes as well. For lake metrics that are comparable between studies, such as allochthonous loading and export, allochthonous water column respiration, and total OC burial, our results were within 20% of values in related studies (Hanson et al. 2014, McCullough et al. 2018).

4.2 Hypolimnetic Respiration

Given the importance of autochthonous POC to hypolimnetic respiration, we assume it contributes substantially to both sediment respiration and respiration in the water column. While previous work found that sediment respiration was the dominant respiration source for lakes with depth ranges encompassed within our study (Steinsberger 2020), we found that water column respiration was at least as important, if not more so. Differences in these findings could be linked to uncertainty in the settling velocity of POC, due to lack of empirical POC settling velocity measurements. Perhaps, POC mineralized in the hypolimnia of our modeled lakes passes more quickly to the sediments in real ecosystems, shifting the balance of respiration more toward the sediments. OC respiration can contribute substantially to hypolimnetic DO depletion in both lakes and reservoirs (Beutel, 2003), and POC settling velocities can be highly variable, suggesting that assumptions around vertical distribution of lake POC deserve further investigation. Another possible explanation for these differences

674 could be that our model missed allochthonous POC loads from extreme events (Carpenter et
675 al., 2012), which can increase the amount of legacy OC stored in the sediments and increase
676 sediment respiration. Our model also does not account for reduced respiration rates due to
677 OC aging, which may explain our higher values of water column respiration. Finally, our
678 model includes entrainment as a possible oxygen source to the hypolimnion, which must be
679 offset by respiration to fit observed hypolimnetic DO changes. Any study that underestimates
680 DO sources to the hypolimnion likely underestimates total respiration.
681
682 Anaerobic mineralization of organic carbon is an important biogeochemical process and can
683 be a substantial carbon sink through methanogenesis (Maerki et al. 2009). Although
684 methanogenesis is not incorporated into our model, methane dissolved in the water column of
685 Lake Mendota is mostly oxidized (Hart 2017), thus contributing to the overall oxygen
686 demand, which is accounted for in our model. What remains unaccounted is ebullition of
687 methane, which is a carbon flux that is difficult to quantify (McClure et al. 2020). Future
688 metabolism studies that include these processes might find a decrease in annual OC burial
689 rates relative to rates in our study. Although we believe that ebullition is not a substantial
690 portion of the lake's carbon mass budget, that remains to be studied more carefully. As the
691 model accounts for DO consumption through calibration, the overall flux would not change
692 even if we link DO consumption to methane oxidation, only the process description would be
693 more realistic.
694

Our findings highlight the importance of autochthonous POC in hypolimnetic oxygen depletion and suggest that related processes, such as the timing of nutrient loading, changes in thermocline depth, or zooplankton grazing, could impact overall lake respiration dynamics and anoxia formation (Schindler et al., 2016; Ladwig et al., 2021; Müller et al., 2012). We also recognize that the DO depletion rate in SP is more uncertain than in the other study lakes. Although we are uncertain of the cause, we speculate that differences in morphometry for this lake could impact the hypolimnetic volume and its capacity to hold DO as well as the rate of sediment oxygen consumption (Livingstone & Imboden 1996). Although lake hypsometry, along with thermal profile, controls the volume of hypolimnion in contact with sediments in our model, there may be other factors related to morphometry (e.g., sediment focusing) that remain unaccounted for, and we see this as an opportunity for future study.

4.3 Long-term Dynamics

Although autochthonous OC dominated the loads across the study lakes, analysis of the long-term OC dynamics supports the importance of allochthony in lakes. Net Ecosystem Production (NEP) has been used to quantify heterotrophy and autotrophy in lakes (Odum 1956, Hanson et al. 2003, Cole et al. 2000, Lovett et al. 2006), and using this metric over multiple decades allowed us to analyze long-term impacts of allochthony. TR, BM, and SP fluctuated between heterotrophy and autotrophy, usually in tandem with trends in hydrology, which acts as a main control of allochthonous OC. This suggests that allochthonous OC inputs may be less important for seasonal anoxia but can still drive a lake toward negative NEP and contribute to sediment carbon storage over long time periods. ME, MO, and AL

717 tended to become less autotrophic over time (Fig. 6), a pattern that coincided with significant
718 decreasing trends in mean epilimnetic total phosphorus concentrations for ME and AL (SI
719 Fig. 5). In our model, NPP and phosphorus are directly related, so decreases in phosphorus
720 are likely to cause decreases in NEP. Short-term respiration of autochthonous POC can
721 account for rapid decreases in hypolimnetic DO, but allochthonous POC, which tends to be
722 more recalcitrant, provides long-term subsidy of ecosystem respiration that can result in
723 long-term net heterotrophy. Thus, it's critical to understand and quantify both the rapid
724 internal cycling based on autochthony and the long and slow turnover of allochthony.
725
726 Through explicitly simulating the cycling of both allochthony and autochthony, we can
727 expand our conceptual model of metabolism to better understand time dynamics of lake
728 water quality at the ecosystem scale. Autochthony has pronounced seasonal dynamics,
729 typically associated with the temporal variability of phytoplankton communities and the
730 growth and senescence of macrophytes (Rautio et al., 2011). While allochthony can also have
731 strong seasonal patterns associated with leaf litter input, pollen blooms, and spring runoff
732 events, its more recalcitrant nature leads to a less pronounced seasonal signal at the
733 ecosystem scale (Wilkinson et al., 2013, Tranvik 1998). When considered together, it seems
734 that allochthony underlies long and slow changes in metabolism patterns, while autochthony
735 overlays strong seasonality. Both OC pools are important for ecosystem scale metabolism
736 processes, and their consequences are evident at different time scales. Therefore, the
737 interactions of both OC sources and their influences on water quality patterns deserve further
738 investigation.

Autochthonous OC control over hypolimnetic respiration should be a primary consideration for understanding the influence of OC on ecosystem dynamics. Hypolimnetic oxygen depletion and anoxia in productive lakes can be mitigated by reducing autochthonous production of OC, which we show is mainly driven by nutrient availability. This study also identifies the need for a better understanding of internal and external OC loads in lakes. Previous studies have found heterotrophic behavior in less productive lakes, but our findings highlight the importance of autochthony in these lakes, especially for shorter-time scale processes that can be missed by looking at broad annual patterns. By using a one-dimensional, two-layer model, we are able to also understand how surface metabolism processes can impact bottom layer dynamics, which would not be possible with a zero-dimensional model. Looking forward, we believe that our understanding of these processes could be improved by building a coupled watershed - metabolism model to more closely explore causal relations between watershed hydrology, nutrient dynamics, and lake morphometry.

Code Availability

Model code and figure creation code are archived in the Environmental Data Initiative repository (https://doi.org/10.6073/PASTA/1B5B947999AA2F9E0E95C91782B36EE9, Delany, 2022).

Data Availability

Driving data, model configuration files, and model result data are archived in the Environmental Data Initiative repository (https://doi.org/10.6073/PASTA/1B5B947999AA2F9E0E95C91782B36EE9, Delany, 2022).

Author Contributions

AD, PH, RL, and CB assisted with model development and analysis of results. AD and PH prepared the manuscript with contributions from RL, CB, and EA.

Competing Interests

The authors declare that they have no conflict of interest.

Acknowledgements:

Funding was provided through the National Science Foundation (NSF), with grants DEB-1753639, DEB-1753657, and DEB-2025982. Funding for Ellen Albright was provided by the NSF Graduate Research Fellowship Program (GRFP), and the Iowa Department of Natural Resources (contract #22CRDLWBMBALM-0002). Funding for Robert Ladwig was provided by the NSF ABI development grant (#DBI 1759865), UW-Madison Data Science Initiative grant, and the NSF HDR grant (#1934633). Data were provided by the North Temperate Lakes Long Term Ecological Research Program and was accessed through the Environmental Data Initiative (DOI: 10.6073/pasta/0dbbfdbcdee623477c000106c444f3fd).

784 References

785 Amon, R. M. W., & Benner, R. (1996). Photochemical and microbial consumption of
786 dissolved organic carbon and dissolved oxygen in the Amazon River system.
787 *Geochimica et Cosmochimica Acta*, *60*(10), 1783–1792. https://doi.org/10.1016/0016-
788 7037(96)00055-5

789 Beutel, M. W. (2003). Hypolimnetic Anoxia and Sediment Oxygen Demand in California
790 Drinking Water Reservoirs. *Lake and Reservoir Management*, *19*(3), 208–221.
791 https://doi.org/10.1080/07438140309354086

792 Bryant, L. D., Hsu-Kim, H., Gantzer, P. A., & Little, J. C. (2011). Solving the problem at the
793 source: Controlling Mn release at the sediment-water interface via hypolimnetic
794 oxygenation. *Water Research*, *45*(19), 6381–6392.
795 https://doi.org/10.1016/j.watres.2011.09.030

796 Cardille, J. A., Carpenter, S. R., Coe, M. T., Foley, J. A., Hanson, P. C., Turner, M. G., &
797 Vano, J. A. (2007). Carbon and water cycling in lake-rich landscapes: Landscape
798 connections, lake hydrology, and biogeochemistry. *Journal of Geophysical Research*,
799 *112*(G2), G02031. https://doi.org/10.1029/2006JG000200

800 Carpenter, S., Arrow, K., Barrett, S., Biggs, R., Brock, W., Crépin, A.-S., Engström, G.,
801 Folke, C., Hughes, T., Kautsky, N., Li, C.-Z., McCarney, G., Meng, K., Mäler, K.-G.,
802 Polasky, S., Scheffer, M., Shogren, J., Sterner, T., Vincent, J., … Zeeuw, A. (2012).
803 General Resilience to Cope with Extreme Events. *Sustainability*, *4*(12), 3248–3259.
804 https://doi.org/10.3390/su4123248

Carpenter, S. R., Benson, B. J., Biggs, R., Chipman, J. W., Foley, J. A., Golding, S. A., Hammer, R. B., Hanson, P. C., Johnson, P. T. J., Kamarainen, A. M., Kratz, T. K., Lathrop, R. C., McMahon, K. D., Provencher, B., Rusak, J. A., Solomon, C. T., Stanley, E. H., Turner, M. G., Vander Zanden, M. J., … Yuan, H. (2007). Understanding Regional Change: A Comparison of Two Lake Districts. *BioScience*, *57*(4), 323–335. https://doi.org/10.1641/B570407

Catalán, N., Marcé, R., Kothawala, D. N., & Tranvik, Lars. J. (2016). Organic carbon decomposition rates controlled by water retention time across inland waters. *Nature Geoscience*, *9*(7), 501–504. https://doi.org/10.1038/ngeo2720

Cole, G., & Weihe, P. (2016). *Textbook of Limnology*. Waveland Press, Inc.

Cole, J. J., & Caraco, N. F. (1998). Atmospheric exchange of carbon dioxide in a low-wind oligotrophic lake measured by the addition of SF_6. *Limnology and Oceanography*, *43*(4), 647–656. https://doi.org/10.4319/lo.1998.43.4.0647

Cole, J. J., Carpenter, S. R., Kitchell, J. F., & Pace, M. L. (2002). Pathways of organic carbon utilization in small lakes: Results from a whole-lake ^{13}C addition and coupled model. *Limnology and Oceanography*, *47*(6), 1664–1675. https://doi.org/10.4319/lo.2002.47.6.1664

Cole, J. J., Pace, M. L., Carpenter, S. R., & Kitchell, J. F. (2000). Persistence of net heterotrophy in lakes during nutrient addition and food web manipulations. *Limnology and Oceanography*, *45*(8), 1718–1730. https://doi.org/10.4319/lo.2000.45.8.1718

826 Creed, I. F., Sanford, S. E., Beall, F. D., Molot, L. A., & Dillon, P. J. (2003). Cryptic
827 wetlands: Integrating hidden wetlands in regression models of the export of dissolved
828 organic carbon from forested landscapes. *Hydrological Processes*, *17*(18), 3629–3648.
829 https://doi.org/10.1002/hyp.1357
830 Delany, A. (2022). *Modeled Organic Carbon, Dissolved Oxygen, and Secchi for six*
831 *Wisconsin Lakes, 1995-2014* [Data set]. Environmental Data Initiative.
832 https://doi.org/10.6073/PASTA/1B5B947999AA2F9E0E95C91782B36EE9
833 Dordoni, M., Seewald, M., Rinke, K., van Geldern, R., Schmidmeier, J., & Barth, J. A. C.
834 (2022). *Mineralization of autochthonous particulate organic carbon is a fast channel of*
835 *organic matter turnover in Germany's largest drinking water reservoir* [Preprint].
836 Biogeochemistry: Stable Isotopes & Other Tracers. https://doi.org/10.5194/bg-
837 2022-154
838 Evans, C. D., Monteith, D. T., & Cooper, D. M. (2005). Long-term increases in surface water
839 dissolved organic carbon: Observations, possible causes and environmental impacts.
840 *Environmental Pollution*, *137*(1), 55–71. https://doi.org/10.1016/j.envpol.2004.12.031
841 Feng, L., Zhang, J., Fan, J., Wei, L., He, S., & Wu, H. (2022). Tracing dissolved organic
842 matter in inflowing rivers of Nansi Lake as a storage reservoir: Implications for water-
843 quality control. *Chemosphere*, *286*, 131624.
844 https://doi.org/10.1016/j.chemosphere.2021.131624
845
846

847 Goudsmit, G.-H., Burchard, H., Peeters, F., & Wüest, A. (2002). Application of k-ϵ
848 turbulence models to enclosed basins: The role of internal seiches: APPLICATION OF
849 k-ϵ TURBULENCE MODELS. *Journal of Geophysical Research: Oceans*, *107*(C12),
850 23-1-23–13. https://doi.org/10.1029/2001JC000954
851 Hanson, P. C., Bade, D. L., Carpenter, S. R., & Kratz, T. K. (2003). Lake metabolism:
852 Relationships with dissolved organic carbon and phosphorus. *Limnology and*
853 *Oceanography*, *48*(3), 1112–1119. https://doi.org/10.4319/lo.2003.48.3.1112
854 Hanson, P.C., Carpenter S.R., Cardille, J.A, Coe, M.T., & Winslow, L.A. (2007). Small lakes
855 dominate a random sample of reginal lake characteristics. *Freshwater Biology* 52(5),
856 814–822. https://doi.org/10.1111/j.1365-2427.2007.01730.x
857 Hanson, P. C., Buffam, I., Rusak, J. A., Stanley, E. H., & Watras, C. (2014). Quantifying lake
858 allochthonous organic carbon budgets using a simple equilibrium model. *Limnology and*
859 *Oceanography*, *59*(1), 167–181. https://doi.org/10.4319/lo.2014.59.1.0167
860 Hanson, P. C., Hamilton, D. P., Stanley, E. H., Preston, N., Langman, O. C., & Kara, E. L.
861 (2011). Fate of Allochthonous Dissolved Organic Carbon in Lakes: A Quantitative
862 Approach. *PLoS ONE*, *6*(7), e21884. https://doi.org/10.1371/journal.pone.0021884
863 Hanson, P. C., Pace, M. L., Carpenter, S. R., Cole, J. J., & Stanley, E. H. (2015). Integrating
864 Landscape Carbon Cycling: Research Needs for Resolving Organic Carbon Budgets of
865 Lakes. *Ecosystems*, *18*(3), 363–375. https://doi.org/10.1007/s10021-014-9826-9
866 Hanson, P. C., Pollard, A. I., Bade, D. L., Predick, K., Carpenter, S. R., & Foley, J. A.
867 (2004). A model of carbon evasion and sedimentation in temperate lakes:

LANDSCAPE-LAKE CARBON CYCLING MODEL. *Global Change Biology*, *10*(8), 1285–1298. https://doi.org/10.1111/j.1529-8817.2003.00805.x

Hanson, P. C., Stillman, A. B., Jia, X., Karpatne, A., Dugan, H. A., Carey, C. C., Stachelek, J., Ward, N. K., Zhang, Y., Read, J. S., & Kumar, V. (2020). Predicting lake surface water phosphorus dynamics using process-guided machine learning. *Ecological Modelling*, *430*, 109136. https://doi.org/10.1016/j.ecolmodel.2020.109136

Hart, J., Dugan, H., Carey, C., Stanley, E., & Hanson, P. (2019). *Lake Mendota Carbon and Greenhouse Gas Measurements at North Temperate Lakes LTER 2016* [Data set]. Environmental Data Initiative. https://doi.org/10.6073/PASTA/170E5BA0ED09FE3D5837EF04C47E432E

Hipsey, M. R. (2022). *Modelling Aquatic Eco-Dynamics: Overview of the AED modular simulation platform*. https://doi.org/10.5281/ZENODO.6516222

Hipsey, M. R., Bruce, L. C., Boon, C., Busch, B., Carey, C. C., Hamilton, D. P., Hanson, P. C., Read, J. S., de Sousa, E., Weber, M., & Winslow, L. A. (2019). A General Lake Model (GLM 3.0) for linking with high-frequency sensor data from the Global Lake Ecological Observatory Network (GLEON). *Geoscientific Model Development*, *12*(1), 473–523. https://doi.org/10.5194/gmd-12-473-2019

Hoffman, A. R., Armstrong, D. E., & Lathrop, R. C. (2013). Influence of phosphorus scavenging by iron in contrasting dimictic lakes. *Canadian Journal of Fisheries and Aquatic Sciences*, *70*(7), 941–952. https://doi.org/10.1139/cjfas-2012-0391

Hotchkiss, E. R., Sadro, S., & Hanson, P. C. (2018). Toward a more integrative perspective on carbon metabolism across lentic and lotic inland waters. *Limnology and Oceanography Letters*, *3*(3), 57–63. https://doi.org/10.1002/lol2.10081

Houser, J. N., Bade, D. L., Cole, J. J., & Pace, M. L. (2003). The dual influences of dissolved organic carbon on hypolimnetic metabolism: Organic substrate and photosynthetic reduction. *Biogeochemistry*, *64*(2), 247–269. https://doi.org/10.1023/A:1024933931691

Hunt, R. J., & Walker, J. F. (2017). *2016 Update to the GSFLOW groundwater-surface water model for the Trout Lake Watershed*. https://doi.org/10.5066/F7M32SZ2

Hunt, R. J., Walker, J. F., Selbig, W. R., Westenbroek, S. M., & Regan, R. S. (2013). *Simulation of Climate-Change Effects on Streamflow, Lake Water Budgets, and Stream Temperature Using GSFLOW and SNTEMP, Trout Lake Watershed, Wisconsin*. United States Geological Survey.

Jane, S. F., Hansen, G. J. A., Kraemer, B. M., Leavitt, P. R., Mincer, J. L., North, R. L., Pilla, R. M., Stetler, J. T., Williamson, C. E., Woolway, R. I., Arvola, L., Chandra, S., DeGasperi, C. L., Diemer, L., Dunalska, J., Erina, O., Flaim, G., Grossart, H.-P., Hambright, K. D., … Rose, K. C. (2021). Widespread deoxygenation of temperate lakes. *Nature*, *594*(7861), 66–70. https://doi.org/10.1038/s41586-021-03550-y

Jansson, M., Bergström, A.-K., Blomqvist, P., & Drakare, S. (2000). ALLOCHTHONOUS ORGANIC CARBON AND PHYTOPLANKTON/BACTERIOPLANKTON PRODUCTION RELATIONSHIPS IN LAKES. *Ecology*, *81*(11), 3250–3255. https://doi.org/10.1890/0012-9658(2000)081[3250:AOCAPB]2.0.CO;2

Jenny, J.-P., Francus, P., Normandeau, A., Lapointe, F., Perga, M.-E., Ojala, A., Schimmelmann, A., & Zolitschka, B. (2016). Global spread of hypoxia in freshwater ecosystems during the last three centuries is caused by rising local human pressure. *Global Change Biology*, *22*(4), 1481–1489. https://doi.org/10.1111/gcb.13193

Jenny, J.-P., Normandeau, A., Francus, P., Taranu, Z. E., Gregory-Eaves, I., Lapointe, F., Jautzy, J., Ojala, A. E. K., Dorioz, J.-M., Schimmelmann, A., & Zolitschka, B. (2016). Urban point sources of nutrients were the leading cause for the historical spread of hypoxia across European lakes. *Proceedings of the National Academy of Sciences*, *113*(45), 12655–12660. https://doi.org/10.1073/pnas.1605480113

Knoll, L. B., Williamson, C. E., Pilla, R. M., Leach, T. H., Brentrup, J. A., & Fisher, T. J. (2018). Browning-related oxygen depletion in an oligotrophic lake. *Inland Waters*, *8*(3), 255–263. https://doi.org/10.1080/20442041.2018.1452355

Kraemer, B. M., Chandra, S., Dell, A. I., Dix, M., Kuusisto, E., Livingstone, D. M., Schladow, S. G., Silow, E., Sitoki, L. M., Tamatamah, R., & McIntyre, P. B. (2017). Global patterns in lake ecosystem responses to warming based on the temperature dependence of metabolism. *Global Change Biology*, *23*(5), 1881–1890. https://doi.org/10.1111/gcb.13459

Ladwig, R., Hanson, P. C., Dugan, H. A., Carey, C. C., Zhang, Y., Shu, L., Duffy, C. J., & Cobourn, K. M. (2021). Lake thermal structure drives interannual variability in summer anoxia dynamics in a eutrophic lake over 37 years. *Hydrology and Earth System Sciences*, *25*(2), 1009–1032. https://doi.org/10.5194/hess-25-1009-2021

931 Lathrop, R., & Carpenter, S. (2014). Water quality implications from three decades of
932 phosphorus loads and trophic dynamics in the Yahara chain of lakes. *Inland Waters*,
933 *4*(1), 1–14. https://doi.org/10.5268/IW-4.1.680
934 Lei, R., Leppäranta, M., Erm, A., Jaatinen, E., & Pärn, O. (2011). Field investigations of
935 apparent optical properties of ice cover in Finnish and Estonian lakes in winter 2009.
936 *Estonian Journal of Earth Sciences*, *60*(1), 50. https://doi.org/10.3176/earth.2011.1.05
937 Livingstone, D. M., & Imboden, D. M. (1996). The prediction of hypolimnetic oxygen
938 profiles: A plea for a deductive approach. *Canadian Journal of Fisheries and Aquatic*
939 *Sciences*, *53*(4), 924–932. https://doi.org/10.1139/f95-230
940 Loose, B., & Schlosser, P. (2011). Sea ice and its effect on CO_2 flux between the atmosphere
941 and the Southern Ocean interior. *Journal of Geophysical Research: Oceans*, *116*(C11),
942 2010JC006509. https://doi.org/10.1029/2010JC006509
943 Lovett, G. M., Cole, J. J., & Pace, M. L. (2006). Is Net Ecosystem Production Equal to
944 Ecosystem Carbon Accumulation? *Ecosystems*, *9*(1), 152–155.
945 https://doi.org/10.1007/s10021-005-0036-3
946 Maerki, M., Müller, B., Dinkel, C., & Wehrli, B. (2009). Mineralization pathways in lake
947 sediments with different oxygen and organic carbon supply. *Limnology and*
948 *Oceanography*, *54*(2), 428–438. https://doi.org/10.4319/lo.2009.54.2.0428
949 Magee, M. R., McIntyre, P. B., Hanson, P. C., & Wu, C. H. (2019). Drivers and Management
950 Implications of Long-Term Cisco Oxythermal Habitat Decline in Lake Mendota, WI.
951 *Environmental Management*, *63*(3), 396–407. https://doi.org/10.1007/s00267-018-
952 01134-7

Magnuson, J., Carpenter, S., & Stanley, E. (2020). *North Temperate Lakes LTER: Chemical Limnology of Primary Study Lakes: Nutrients, pH and Carbon 1981 - current* [Data set]. Environmental Data Initiative. https://doi.org/10.6073/PASTA/8359D27BBD91028F222D923A7936077D

Magnuson, J. J., Benson, B. J., & Kratz, T. K. (2006). *Long-term dynamics of lakes in the landscape: Long-term ecological research on north temperate lakes.* Oxford University Press on Demand.

Magnuson, J. J., Carpenter, S. R., & Stanley, E. H. (2022). *North Temperate Lakes LTER: Physical Limnology of Primary Study Lakes 1981 - current* [Data set]. Environmental Data Initiative. https://doi.org/10.6073/PASTA/925D94173F35471F699B5BC343AA1128

McClure, R. P., Lofton, M. E., Chen, S., Krueger, K. M., Little, J. C., & Carey, C. C. (2020). The Magnitude and Drivers of Methane Ebullition and Diffusion Vary on a Longitudinal Gradient in a Small Freshwater Reservoir. *Journal of Geophysical Research: Biogeosciences*, *125*(3). https://doi.org/10.1029/2019JG005205

McCullough, I. M., Dugan, H. A., Farrell, K. J., Morales-Williams, A. M., Ouyang, Z., Roberts, D., Scordo, F., Bartlett, S. L., Burke, S. M., Doubek, J. P., Krivak-Tetley, F. E., Skaff, N. K., Summers, J. C., Weathers, K. C., & Hanson, P. C. (2018). Dynamic modeling of organic carbon fates in lake ecosystems. *Ecological Modelling*, *386*, 71–82. https://doi.org/10.1016/j.ecolmodel.2018.08.009

Mi, C., Shatwell, T., Ma, J., Wentzky, V. C., Boehrer, B., Xu, Y., & Rinke, K. (2020). The formation of a metalimnetic oxygen minimum exemplifies how ecosystem dynamics shape biogeochemical processes: A modelling study. *Water Research*, *175*, 115701. https://doi.org/10.1016/j.watres.2020.115701

Morris, M. D. (1991). Factorial Sampling Plans for Preliminary Computational Experiments. *Technometrics*, *33*(2), 161–174. https://doi.org/10.1080/00401706.1991.10484804

Müller, B., Bryant, L. D., Matzinger, A., & Wüest, A. (2012). Hypolimnetic Oxygen Depletion in Eutrophic Lakes. *Environmental Science & Technology*, *46*(18), 9964–9971. https://doi.org/10.1021/es301422r

Nürnberg, G. K. (1995). Quantifying anoxia in lakes. *Limnology and Oceanography*, *40*(6), 1100–1111. https://doi.org/10.4319/lo.1995.40.6.1100

Odum, H. T. (1956). Primary Production in Flowing Waters. *Limnology and Oceanography*, *1*(2), 102–117. https://doi.org/10.4319/lo.1956.1.2.0102

Platt, T., Gallegos, C., & Harrison, W. (1980). Photoinhibition of photosynthesis in natural assemblages of marine phytoplankton. *Journal of Marine Research*, *38*(4), 687–701.

Prairie, Y. T., Bird, D. F., & Cole, J. J. (2002). The summer metabolic balance in the epilimnion of southeastern Quebec lakes. *Limnology and Oceanography*, *47*(1), 316–321. https://doi.org/10.4319/lo.2002.47.1.0316

Qu, Y., & Duffy, C. J. (2007). A semidiscrete finite volume formulation for multiprocess watershed simulation: MULTIPROCESS WATERSHED SIMULATION. *Water Resources Research*, *43*(8). https://doi.org/10.1029/2006WR005752

997 Rautio, M., Mariash, H., & Forsström, L. (2011). Seasonal shifts between autochthonous and
998 allochthonous carbon contributions to zooplankton diets in a subarctic lake. *Limnology*
999 *and Oceanography*, *56*(4), 1513–1524. https://doi.org/10.4319/lo.2011.56.4.1513
1000 Read, E. K., Ivancic, M., Hanson, P., Cade-Menun, B. J., & McMahon, K. D. (2014).
1001 Phosphorus speciation in a eutrophic lake by 31P NMR spectroscopy. *Water Research*,
1002 *62*, 229–240. https://doi.org/10.1016/j.watres.2014.06.005
1003 Read, J. S., Hamilton, D. P., Jones, I. D., Muraoka, K., Winslow, L. A., Kroiss, R., Wu, C.
1004 H., & Gaiser, E. (2011). Derivation of lake mixing and stratification indices from high-
1005 resolution lake buoy data. *Environmental Modelling & Software*, *26*(11), 1325–1336.
1006 https://doi.org/10.1016/j.envsoft.2011.05.006
1007 Read, J. S., Zwart, J. A., Kundel, H., Corson-Dosch, H. R., Hansen, G. J. A., Vitense, K.,
1008 Appling, A. P., Oliver, S. K., & Platt, L. (2021). *Data release: Process-based*
1009 *predictions of lake water temperature in the Midwest US* [Data set]. U.S. Geological
1010 Survey. https://doi.org/10.5066/P9CA6XP8
1011 Reynolds, C. S., Oliver, R. L., & Walsby, A. E. (1987). Cyanobacterial dominance: The role
1012 of buoyancy regulation in dynamic lake environments. *New Zealand Journal of Marine*
1013 *and Freshwater Research*, *21*(3), 379–390.
1014 https://doi.org/10.1080/00288330.1987.9516234
1015 Rhodes, J., Hetzenauer, H., Frassl, M. A., Rothhaupt, K.-O., & Rinke, K. (2017). Long-term
1016 development of hypolimnetic oxygen depletion rates in the large Lake Constance.
1017 *Ambio*, *46*(5), 554–565. https://doi.org/10.1007/s13280-017-0896-8

1018 Richardson, D. C., Carey, C. C., Bruesewitz, D. A., & Weathers, K. C. (2017). Intra- and
1019 inter-annual variability in metabolism in an oligotrophic lake. *Aquatic Sciences*, *79*(2),
1020 319–333. https://doi.org/10.1007/s00027-016-0499-7
1021 Rippey, B., & McSorley, C. (2009). Oxygen depletion in lake hypolimnia. *Limnology and*
1022 *Oceanography*, *54*(3), 905–916. https://doi.org/10.4319/lo.2009.54.3.0905
1023 Schindler, D. W., Carpenter, S. R., Chapra, S. C., Hecky, R. E., & Orihel, D. M. (2016).
1024 Reducing Phosphorus to Curb Lake Eutrophication is a Success. *Environmental Science*
1025 *& Technology*, *50*(17), 8923–8929. https://doi.org/10.1021/acs.est.6b02204
1026 Snortheim, C. A., Hanson, P. C., McMahon, K. D., Read, J. S., Carey, C. C., & Dugan, H. A.
1027 (2017). Meteorological drivers of hypolimnetic anoxia in a eutrophic, north temperate
1028 lake. *Ecological Modelling*, *343*, 39–53.
1029 https://doi.org/10.1016/j.ecolmodel.2016.10.014
1030 Sobek, S., Tranvik, L. J., Prairie, Y. T., Kortelainen, P., & Cole, J. J. (2007). Patterns and
1031 regulation of dissolved organic carbon: An analysis of 7,500 widely distributed lakes.
1032 *Limnology and Oceanography*, *52*(3), 1208–1219.
1033 https://doi.org/10.4319/lo.2007.52.3.1208
1034 Soetaert, K., & Petzoldt, T. (2010). Inverse Modelling, Sensitivity and Monte Carlo Analysis
1035 in *R* Using Package **FME**. *Journal of Statistical Software*, *33*(3).
1036 https://doi.org/10.18637/jss.v033.i03
1037 Solomon, C. T., Bruesewitz, D. A., Richardson, D. C., Rose, K. C., Van De Bogert, M. C.,
1038 Hanson, P. C., Kratz, T. K., Larget, B., Adrian, R., Babin, B. L., Chiu, C.-Y., Hamilton,
1039 D. P., Gaiser, E. E., Hendricks, S., Istvànovics, V., Laas, A., O'Donnell, D. M., Pace, M.

L., Ryder, E., … Zhu, G. (2013). Ecosystem respiration: Drivers of daily variability and background respiration in lakes around the globe. *Limnology and Oceanography*, *58*(3), 849–866. https://doi.org/10.4319/lo.2013.58.3.0849

Solomon, C. T., Jones, S. E., Weidel, B. C., Buffam, I., Fork, M. L., Karlsson, J., Larsen, S., Lennon, J. T., Read, J. S., Sadro, S., & Saros, J. E. (2015). Ecosystem Consequences of Changing Inputs of Terrestrial Dissolved Organic Matter to Lakes: Current Knowledge and Future Challenges. *Ecosystems*, *18*(3), 376–389. https://doi.org/10.1007/s10021-015-9848-y

Soranno, P. A., Carpenter, S. R., & Lathrop, R. C. (1997). Internal phosphorus loading in Lake Mendota: Response to external loads and weather. *Canadian Journal of Fisheries and Aquatic Sciences*, *54*(8), 1883–1893. https://doi.org/10.1139/f97-095

Staehr, P. A., Bade, D., Van de Bogert, M. C., Koch, G. R., Williamson, C., Hanson, P., Cole, J. J., & Kratz, T. (2010). Lake metabolism and the diel oxygen technique: State of the science: Guideline for lake metabolism studies. *Limnology and Oceanography: Methods*, *8*(11), 628–644. https://doi.org/10.4319/lom.2010.8.0628

Steinsberger, T., Schwefel, R., Wüest, A., & Müller, B. (2020). Hypolimnetic oxygen depletion rates in deep lakes: Effects of trophic state and organic matter accumulation. *Limnology and Oceanography*, *65*(12), 3128–3138. https://doi.org/10.1002/lno.11578

Thorp, J. H., & Delong, M. D. (2002). Dominance of autochthonous autotrophic carbon in food webs of heterotrophic rivers. *Oikos*, *96*(3), 543–550. https://doi.org/10.1034/j.1600-0706.2002.960315.x

1061 Toming, K., Kotta, J., Uuemaa, E., Sobek, S., Kutser, T., & Tranvik, L. J. (2020). Predicting
1062 lake dissolved organic carbon at a global scale. *Scientific Reports*, *10*(1), 8471.
1063 https://doi.org/10.1038/s41598-020-65010-3
1064 Tranvik, L. J. (1998). Degradation of Dissolved Organic Matter in Humic Waters by
1065 Bacteria. In D. O. Hessen & L. J. Tranvik (Eds.), *Aquatic Humic Substances* (Vol. 133,
1066 pp. 259–283). Springer Berlin Heidelberg. https://doi.org/10.1007/978-3-662-03736-
1067 2_11
1068 Webster, K. E., Kratz, T. K., Bowser, C. J., Magnuson, J. J., & Rose, W. J. (1996). The
1069 influence of landscape position on lake chemical responses to drought in northern
1070 Wisconsin. *Limnology and Oceanography*, *41*(5), 977–984.
1071 https://doi.org/10.4319/lo.1996.41.5.0977
1072 Wilkinson, G. M., Pace, M. L., & Cole, J. J. (2013). Terrestrial dominance of organic matter
1073 in north temperate lakes: ORGANIC MATTER COMPOSITION IN LAKES. *Global*
1074 *Biogeochemical Cycles*, *27*(1), 43–51. https://doi.org/10.1029/2012GB004453
1075 Williamson, C. E., Dodds, W., Kratz, T. K., & Palmer, M. A. (2008). Lakes and streams as
1076 sentinels of environmental change in terrestrial and atmospheric processes. *Frontiers in*
1077 *Ecology and the Environment*, *6*(5), 247–254. https://doi.org/10.1890/070140
1078 Winslow, L. A., Zwart, J. A., Batt, R. D., Dugan, H. A., Woolway, R. I., Corman, J. R.,
1079 Hanson, P. C., & Read, J. S. (2016). LakeMetabolizer: An R package for estimating lake
1080 metabolism from free-water oxygen using diverse statistical models. *Inland Waters*,
1081 *6*(4), 622–636. https://doi.org/10.1080/IW-6.4.883
1082